OPTICAL CONSTANTS OF FULLY IONIZED PLASMAS FOR THE RADIATION OF RUBY, NEODYMIUM-GLASS, AND CO_2 LASERS

Heinrich Hora, Hannelore Müller

3/81
6/71

November 1968

INSTITUT FÜR PLASMAPHYSIK

GARCHING BEI MÜNCHEN

INSTITUT FÜR PLASMAPHYSIK

GARCHING BEI MÜNCHEN

OPTICAL CONSTANTS OF FULLY IONIZED PLASMAS FOR THE RADIATION OF RUBY, NEODYMIUM-GLASS, AND CO_2 LASERS

Heinrich Hora, Hannelore Müller

3/81
6/71

November 1968

Die nachstehende Arbeit wurde im Rahmen des Vertrages zwischen dem Institut für Plasmaphysik GmbH und der Europäischen Atomgemeinschaft über die Zusammenarbeit auf dem Gebiete der Plasmaphysik durchgeführt.

IPP 3/81 Heinrich Hora
6/71 Hannelore Müller

Optical constants of fully ionized plasmas for the radiation of ruby, neodymium-glass, and CO_2 lasers

(in English)

Abstract

The refractive index n and the absorption constant K are numerically evaluated for fully ionized plasmas with atomic numbers Z = 1 to 4 as functions of the electron temperature T and atomic density N for the case of ruby, neodymium-glass, and CO_2 laser radiation and for the second harmonics of each type of radiation on the basis of the two-fluid model of hydrodynamics using Spitzer's collision frequency ν .

Since the first successful measurement of laser light scattering by plasmas[1] and the advent of plasma production by lasers for the purpose of controlled thermonuclear reactions[2], knowledge of the plasmas at the frequencies of laser radiation has become increasingly important. A detailed evaluation of the optical constants of the lasers of the two-fluid model[3] has already been given[4)5)] using the electron collision frequency ν of Spitzer[6]. Comparison with the theory of the optical constants of Dawson and Oberman[7] and of the inverse bremsstrahlung theory[8] shows agreement within a factor of about 2 to 3. While the bremsstrahlung theory is only valid for electron densities N_e [cm^{-3}] which give a plasma frequency ω_p

$$\omega_p^2 = \frac{4\pi N_e e^2}{m_e} \quad sec^{-2} \qquad (1)$$

(e ~ electron charge = 4.812×10^{-10} cgs)

(m_e ~ electron mass = 9.108×10^{-28} g)

much smaller than the radian frequency ω of the incident electromagnetic radiation, the Dawson-Oberman theory and the two-fluid model also give the optical constants for overdense ($\omega_p > \omega$) plasmas. The fairly good agreement obtained between the values in the overdense case[5] by these essentially different treatments justifies using the collision frequency in the high-frequency case of the two-fluid model though ν was derived from the low-frequency conductivity of plasmas[6].

For practical applications of the optical constants of plasmas, the formula of the two-fluid model was appropriate in several cases[9] to [18]. A relatively simple way is given for purposes of numerical programming, especially with respect to using exact values in the overdense case, since it was necessary to study the thermokinetic expansion properties of plasmas produced by lasers from free-falling solid specks[19]. An other way of overcoming the complications of overdense plasmas[20] is to take the approximation formula of the optical constants for low densities, as given by Dawson and Oberman[7] or, in the same way, to apply the

bremsstrahlung theory[8] or the two-fluid model[5], and use for overdense properties a certain metallic absorption constant. The overdense properties of a plasma surface have also been studied with respect to the relaxation mechanisms associated with the absorption process[21].

Limitations on applying the usual optical constants are imposed by nonlinear effects at high laser intensities. One of these effects is interaction between the electromagnetic field and an inhomogeneous plasma, which produced a time averaged acceleration[22)23)24)]. Discussion of the importance of this process is still in the early stage. Under the conditions of the lasers available at present, the process is of comparable magnitude inside of plasmas if an important denominator is not neglected in an estimation of special case[25]. Furthermore the mentioned nonlinear process should govern the observed nonlinear[26)27)] surface acceleration[28] of laser produced plasmas. An other nonlinear effect is the decrease[29)30)] of the collision frequency ν at high intensities where the oscillation energy of the electrons in the electromagnetic field attains the magnitude of the thermal energy kT of the electrons. The maximum electric field strength E_o of the radiation which produces an oscillation energy equal to the value kT is given by

$$E_o = \sqrt{\frac{4m\omega^2}{e^2} kT} \quad , \text{ which} \tag{2}$$

for ruby lasers ($[E_o]$ = V/cm; $[T]$ = eV), is

$$E_o = 1.263 \times 10^8 \sqrt{T} \tag{3}$$

for neodymium-glass lasers

$$E_o = 8.27 \times 10^7 \sqrt{T} \tag{4}$$

for CO_2 lasers

$$E_o = 8.27 \times 10^6 \sqrt{T} \tag{5}$$

The complex refractive index $\tilde{n}$ for a plasma without external magnetic fields is found from the Maxwellian equations and the equations of the two-fluid model without pressure terms and neglecting relativistic motions of the plasma to be

$$\tilde{n}^2 = 1 - \frac{\omega_p^2}{\omega^2} \frac{1}{1 - i\frac{\nu}{\omega}} \tag{6}$$

Spatial inhomogeneities are covered very generally by the expression (6). The electron collision frequency of Spitzer[6] in Gaussian units is

$$\nu = \frac{\omega_p^2 \pi^{3/2} m_e^{1/2} Z e^2 \ln\Lambda}{8\pi \gamma_E(Z) (2kT)^{3/2}} \tag{7}$$

where we have used the atomic number Z of the fully ionized plasma, Spitzer's correction $\gamma_E(Z)$[6], and the Coulomb logarithm

$$\Lambda = \frac{3}{2Ze^3} \left(\frac{k^3 T^3}{\pi N_e} \right)^{1/2}. \tag{8}$$

With $[N_e] = \mathrm{cm}^{-3}$ and $[T] = \mathrm{eV}$ we obtain

$$\nu = \frac{8.64 \times 10^{-7}}{\gamma_E(Z)} \frac{Z N_e}{T^{3/2}} \ln\left(1.555 \times 10^{10} \frac{T^{3/2}}{Z N_e} \right), \tag{9}$$

which is slightly more general than before[4] and where the values[6] $\gamma_E(1) = 0.582$; $\gamma_E(2) = 0.683$; $\gamma_E(3) = 0.744$; $\gamma_E(4) = 0.785$.

The real part of $\tilde{n}$, the refractive index n, is found from (6) to be

$$n = \sqrt{\frac{1}{2}\left\{\sqrt{\left(1-\frac{\omega_p^2}{\omega^2+\nu^2}\right)^2+\left(\frac{\nu}{\omega}\frac{\omega_p^2}{\omega^2+\nu^2}\right)^2}+1-\frac{\omega_p^2}{\omega^2+\nu^2}\right\}} \qquad (10)$$

The imaginary part of $\tilde{n}$ is the absorption coefficient $\varkappa$, which we express by the absorption constant K:

$$K = 2\frac{\omega}{c}\varkappa = 2\frac{\omega}{c}\sqrt{\frac{1}{2}\left\{\sqrt{\left(1-\frac{\omega_p^2}{\omega^2+\nu^2}\right)^2+\left(\frac{\nu}{\omega}\frac{\omega_p^2}{\omega^2+\nu^2}\right)^2}-1+\frac{\omega_p^2}{\omega^2+\nu^2}\right\}} \qquad (11)$$

The simple meaning of K can be seen in the special case of a homogeneous plasma from the attenuation of the intensity I of the electromagnetic radiation propagating along x

$$I = I_0 e^{-Kx} \qquad (12)$$

The following plots give a numerical evaluation of n and K for Z = 1 to 4 for the case of ruby, neodymium-glass, and CO_2 laser radiation and for the second harmonics of each of these types of radiation. As it was done in the plots before[5], the curves of n and $\varkappa$ as a function of the electron temperature T for different atomic densities N are drawn continuously in cases where the Boltzmann statistics are valid, while the dashed curves show the range of conditions of Fermi statistics which may disturb our assumptions of the collision frequency ν. The curves terminate at low temperatures under conditions where the Coulomb logarithm reaches the value 1. Under such conditions the assumption of the full ionisation of the plasma is no longer valid.

References

1) E. Fünfer, B. Kronast, and H.J. Kunze, Phys. Letters 5, 125 (1963)

2) N.G. Basov, and O.N. Krokhin, Proceedings of the Conference on Quantum Electronics, Paris 1963

3) A. Schlüter, Z. Naturforsch. 5a, 72 (1950)

4) H.Hora, Institut für Plasmaphysik, Garching, Report 6/23 (1964); USAEC-Rep. NRC-TT 1193 (1965)

5) H. Hora, Institut für Plasmaphysik, Garching, Report 6/27

6) L. Spitzer, jr., Physics of Fully Ionized Gases, Interscience, New York 1956

7) J.M. Dawson, and C. Oberman, Phys. Fluids, 5, 517 (1962)

8) See, for example, C.W. Allen,Astrophysical Quantities, Athlon Press, London 1955

9) H.J. Kunze, Z. Naturforsch. 20A, 801 (1965)

10) Phillip N. Mace, Los Alamos Scientific Laboratories, Report 3369-UC-34, Phys. TID-4500 (1965)

11) A. Salat, Institut für Plasmaphysik, Garching, Report 6/49 (1966)

12) H. Opower, and W. Press, Z. Naturforsch. 21A, 344 (1966)

13) A.F. Haught, and D.H. Polk, Phys. Fluids 9, 2047 (1966)

14) A.G. Engelhardt, Westinghouse Research Rept., WERL-3472-5 (1967)

15) H. Opower, H. Puell, W. Heinicke, and W. Kaiser, Z. Naturforsch. 22A, 1392 (1967)

16) A. Cavaliere, P. Giupponi, and R. Gratton, Phys. Letters 25A, 636 (1967)

17) K.H. Sun, J.M. Hicks, L.M Epstein, and E.W. Sucov, J. Appl. Phys. 38, 3402 (1967)

18) D.K. Bhadra, Phys. Fluids, 11, 234 (1968)

19) T.V. George, A.G. Engelhardt, J.L. Pack, H. Hora, and G. Cox, Paper presented at the Meeting of the APS Division of Plasma Physics, Miami, Fa. Nov. 16, 1968

20) P. Mulser, and S. Witkowski, Institut für Plasmaphysik, Garching, Report 3/74 (1968)

21) J. Dawson, P. Kaw, and B. Green, AIAA Symposium Los Angeles, June 24-26, 1968

22) H.Hora, D. Pfirsch, and A. Schlüter, Z. Naturforsch. 22A, 278, (1967)

23) A. Schlüter, Plasma Physics 10, 471 (1968)

24) H. Hora, Westinghouse Research Paper 68-IE5-PLASL-P3, May 1968, Phys. Fluids (to be published)

25) A.F. Haught, D.H. Polk, and W.J. Fader, UARL-Report G 920365-9 (July 1968)

26) N.R. Isenor, Appl. Phys. Letters 4, 152 (1964)

27) S. Namba, P.H. Kim, T. Itoh, T. Arai, and H. Schwarz, Record of the IEEE 9th Annual Symposium on Electron, Ion and Laser Beam Technology, Berkeley 9-11 May 1967 (R.F.W. Pease, Editor) San Francisco Press 1967, p. 86

29) R.K. Kaw, and A.R. Salat, Princeton University MATT-Report 598 (April 1968) (to be published)

30) R.E. Kidder, Paper presented at the AIAA Symposium on Laser Produced Plasmas, Los Angeles, Calif., 24 June, 1968.

List of Figures

Ruby laser Fig. 1 to 16

laser frequency: Fig. 1 to 8

Z = 1 (H): n Fig. 1; K Fig. 2
Z = 2 (He): n Fig. 3; K Fig. 4
Z = 3 (Li): n Fig. 5; K Fig. 6
Z = 4 (Be): n Fig. 7; K Fig. 8

second harmonics: Fig. 9 to 16

Z = 1 (H): n Fig. 9; K Fig. 10
Z = 2 (He): n Fig. 11; K Fig. 12
Z = 3 (Li): n Fig. 13; K Fig. 14
Z = 4 (Be): n Fig. 15; K Fig. 16

Neodymium glass laser Fig. 17 to 32

laser frequency: Fig. 17 to 24

Z = 1 (H): n Fig. 17; K Fig. 18
Z = 2 (He): n Fig. 19; K Fig. 20
Z = 3 (Li): n Fig. 21; K Fig. 22
Z = 4 (Be): n Fig. 23; K Fig. 24

second harmonics: Fig. 25 to 32

Z = 1 (H): n Fig. 25; K Fig. 26
Z = 2 (He): n Fig. 27; K Fig. 28
Z = 3 (Li): n Fig. 29; K Fig. 30
Z = 4 (Be): n Fig. 31; K Fig. 32

CO_2 laser Fig. 33 to 40

laser frequency: Fig. 33 to 40

Z = 1 (H): n Fig. 33; K Fig. 34
Z = 2 (He): n Fig. 35; K Fig. 36
Z = 3 (Li): n Fig. 37; K Fig. 38
Z = 4 (Be): n Fig. 39; K Fig. 40

second harmonics:

Z = 1 (H): n Fig. 41; K Fig. 42
Z = 2 (He): n Fig. 43; K Fig. 44
Z = 3 (Li): n Fig. 45; K Fig. 46
Z = 4 (Be): n Fig. 47; K Fig. 48

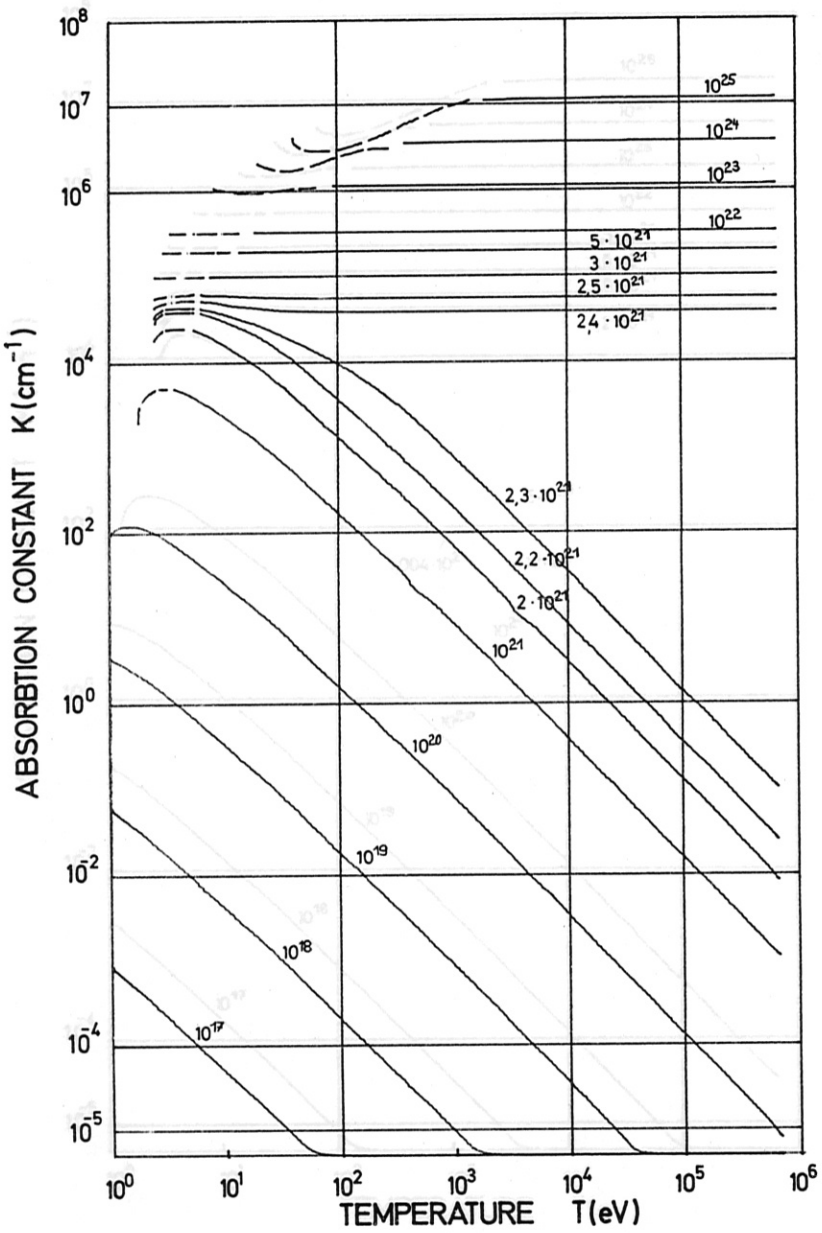

Fig. 1 Absorption constant K for ruby laser radiation as a function of the electron temperature T and atomic densities N for full ionization with Z = 1 (hydrogen).

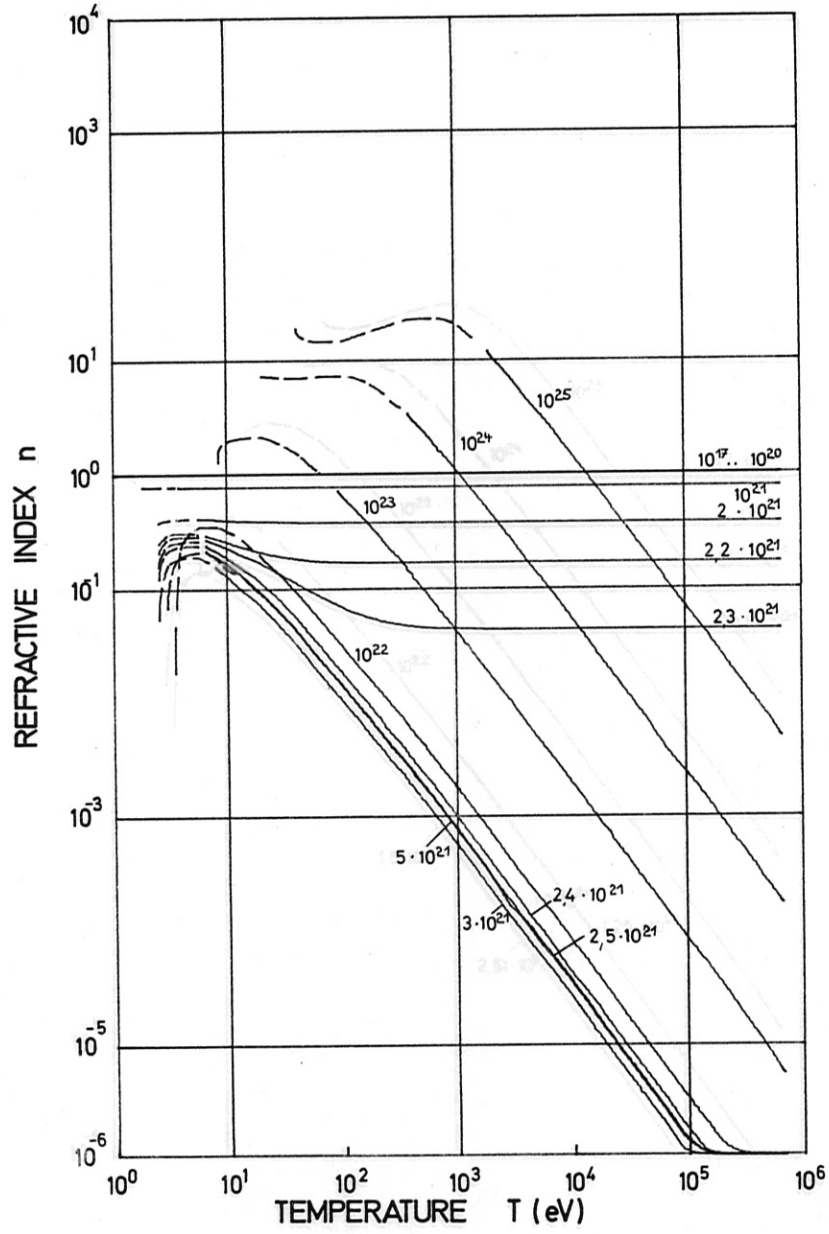

Fig. 2 Refractive index n for ruby laser radiation as a function of the electron temperature T and atomic densities N for full ionization with Z = 1 (hydrogen).

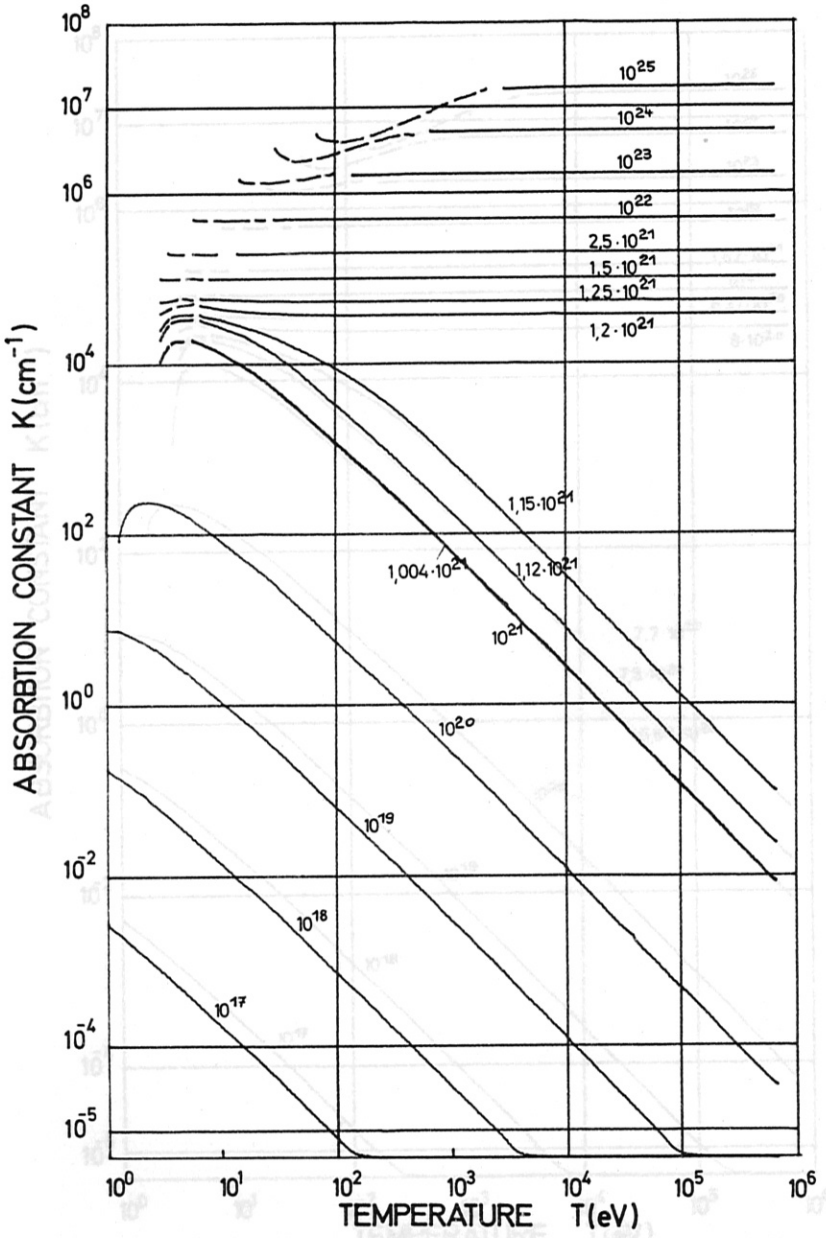

Fig. 3 Absorption constant K for ruby laser radiation as a function of the electron temperature T and atomic densities N for full ionization with Z = 2 (helium).

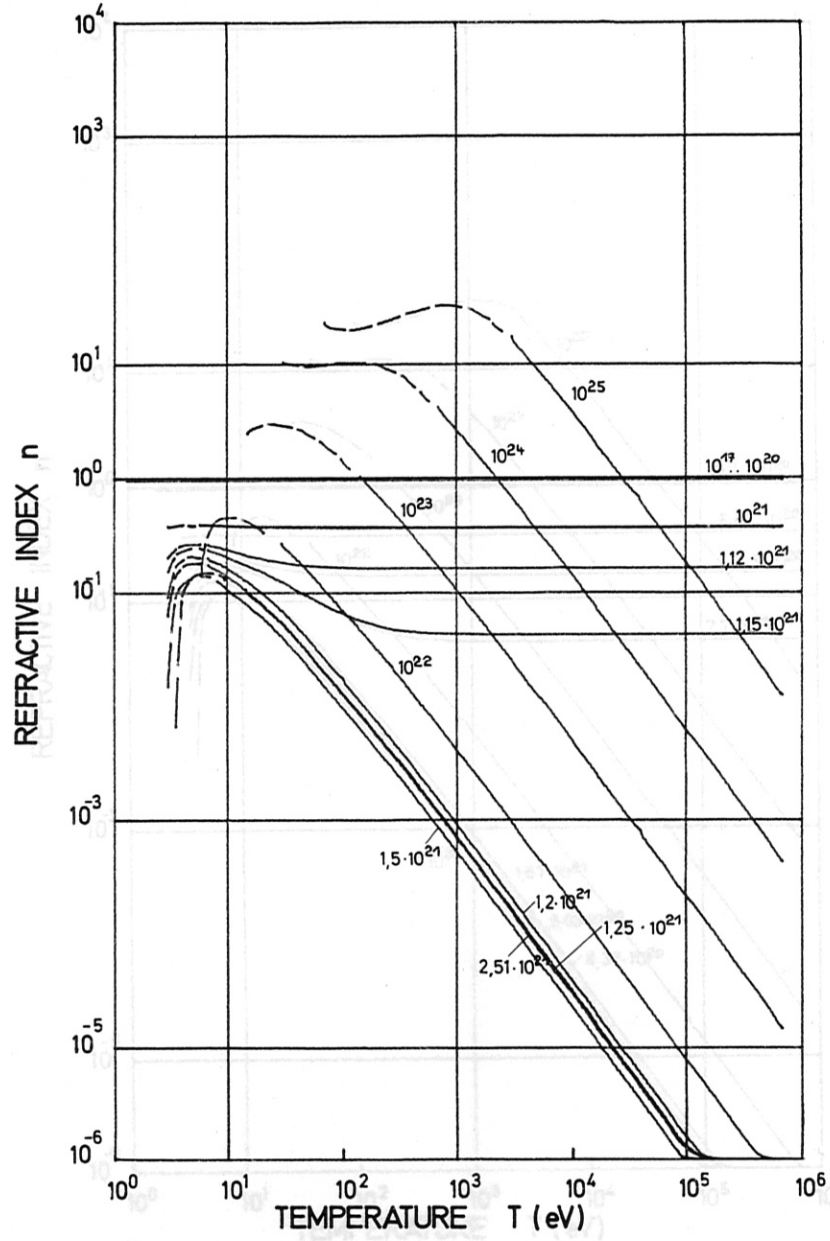

Fig. 4 Refractive index n for ruby laser radiation as a function of the electron temperature T and atomic densities N for full ionization with Z = 2 (helium).

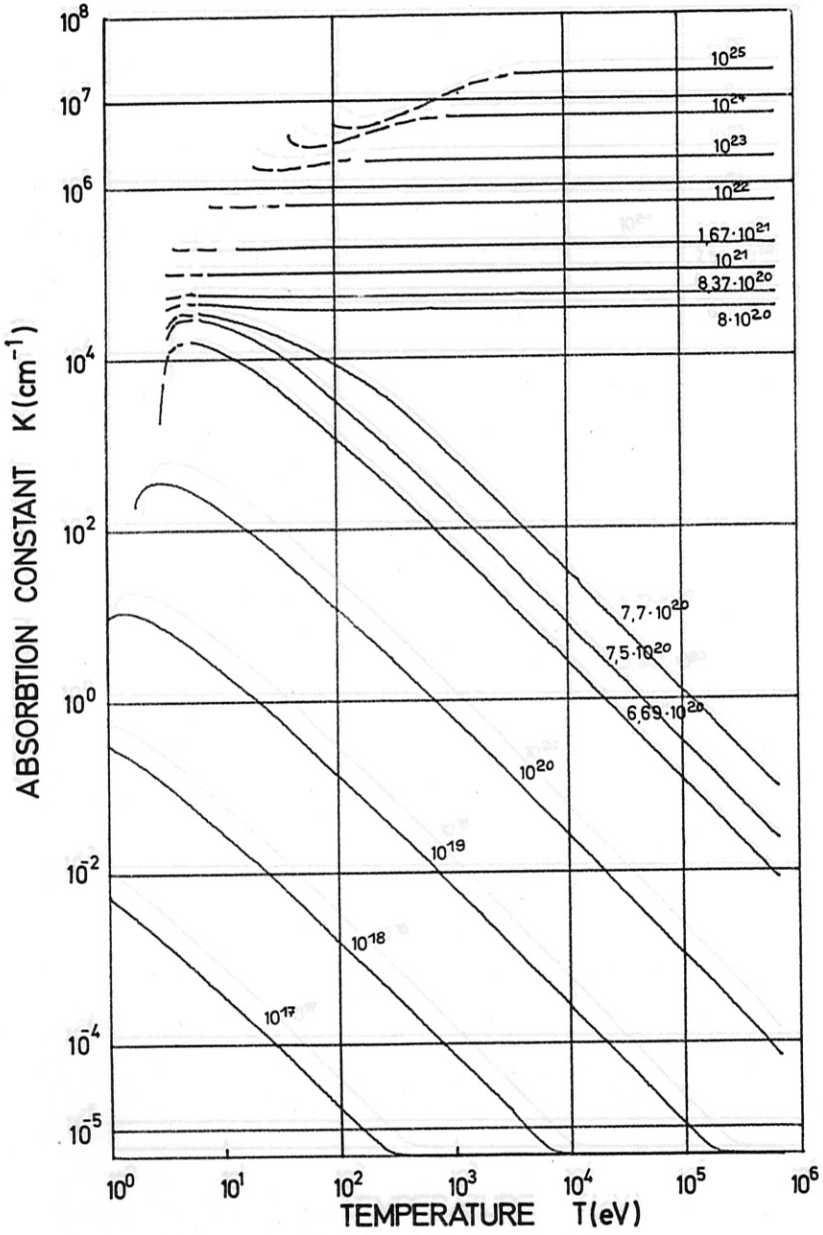

Fig. 5 Absorption constant K for ruby laser radiation as a function of the electron temperature T and atomic densities N for full ionization with Z = 3 (lithium).

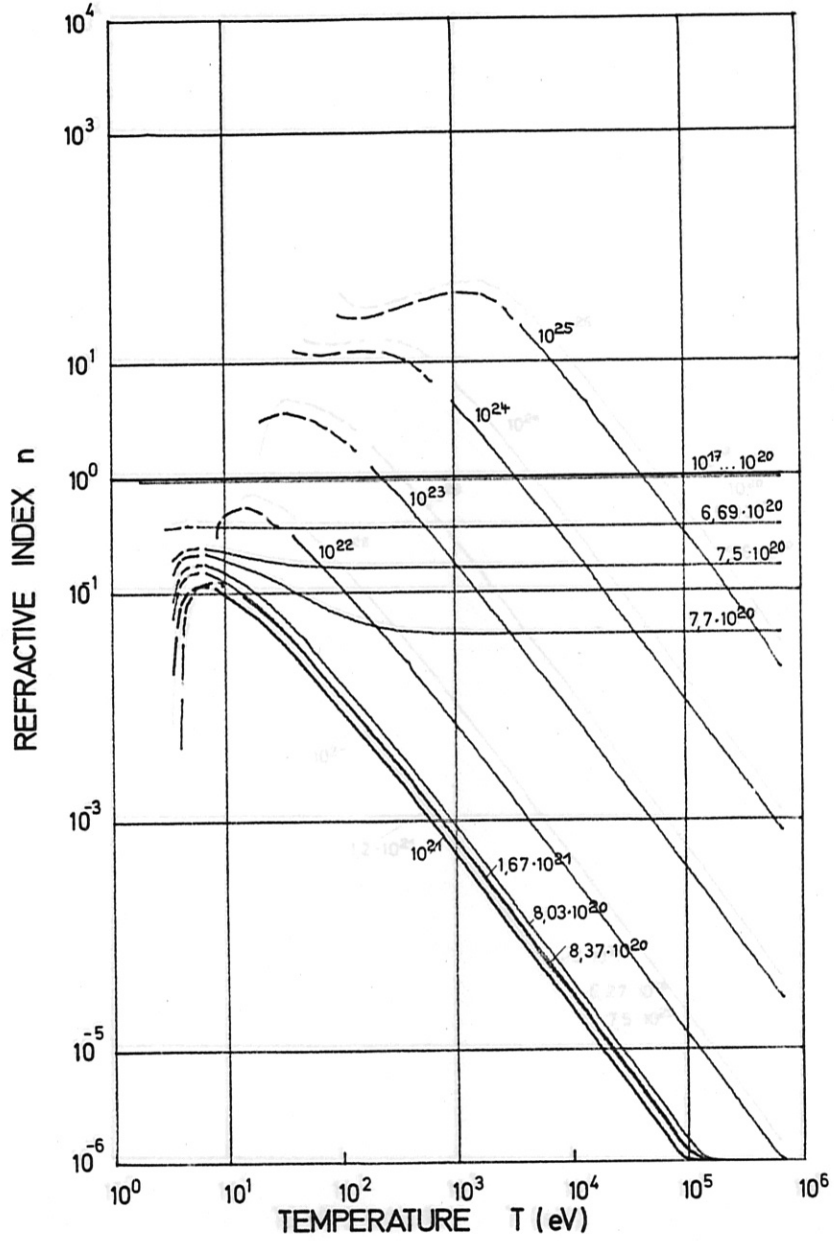

Fig. 6 Refractive index n for ruby laser radiation as a function of the electron temperature T and atomic densities N for full ionization with Z = 3 (lithium).

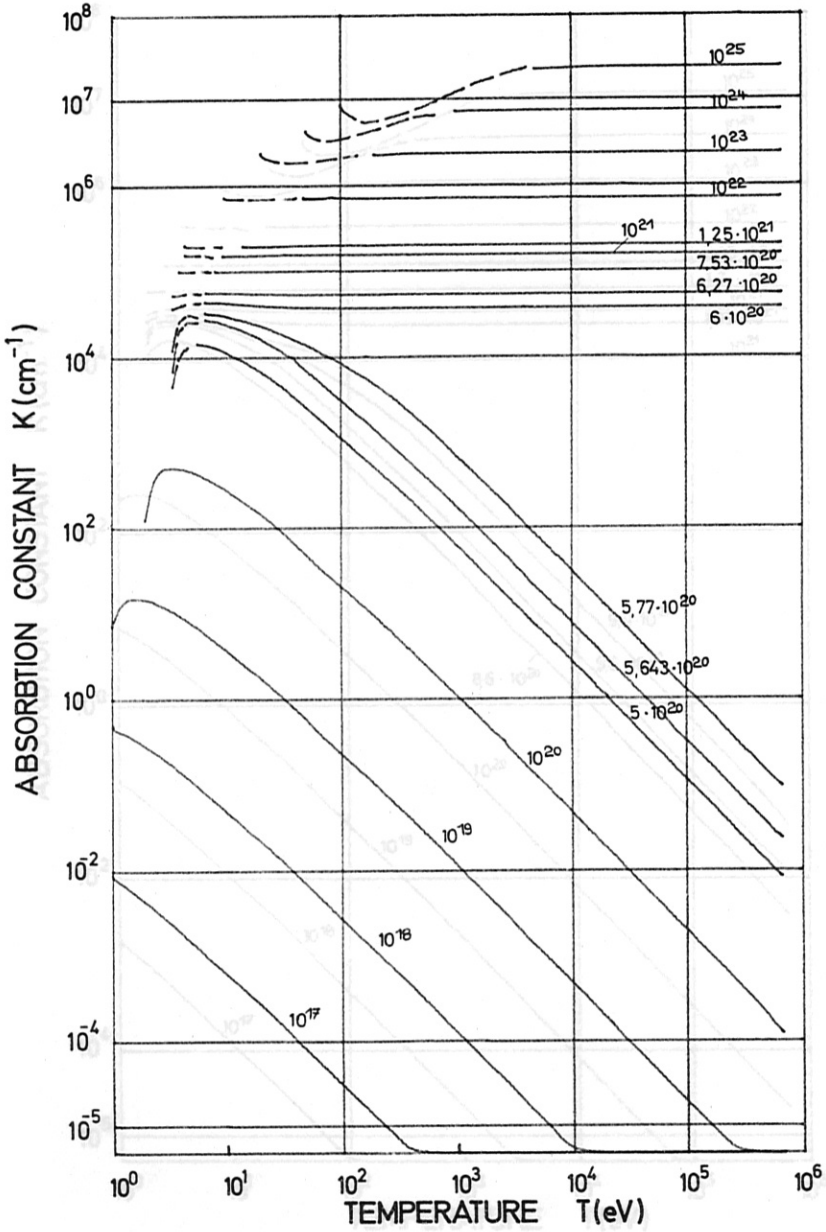

Fig. 7 Absorption constant K for ruby laser radiation as a function of the electron temperature T and atomic densities N for full ionization with Z = 4 (beryllium).

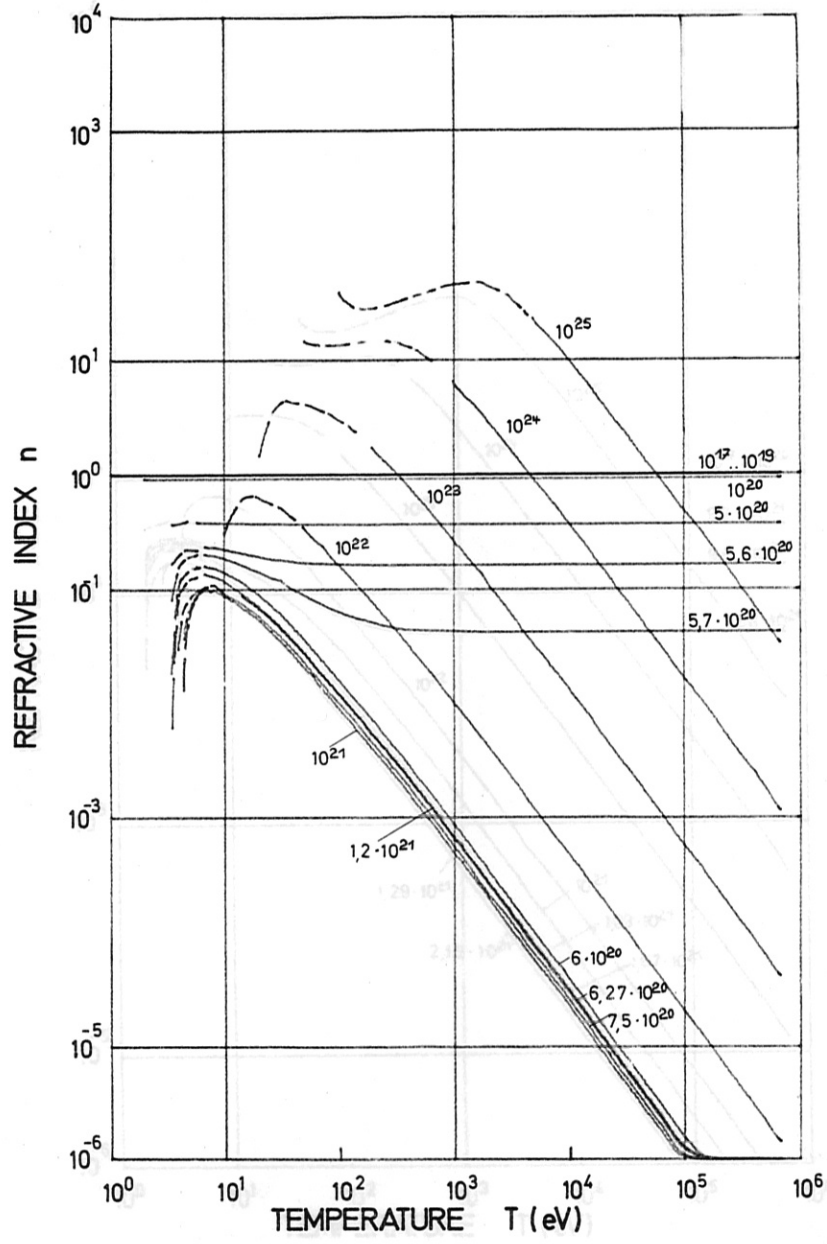

Fig. 8 Refractive index n for ruby laser radiation as a function of the electron temperature T and atomic densities N for full ionization with Z = 4 (beryllium).

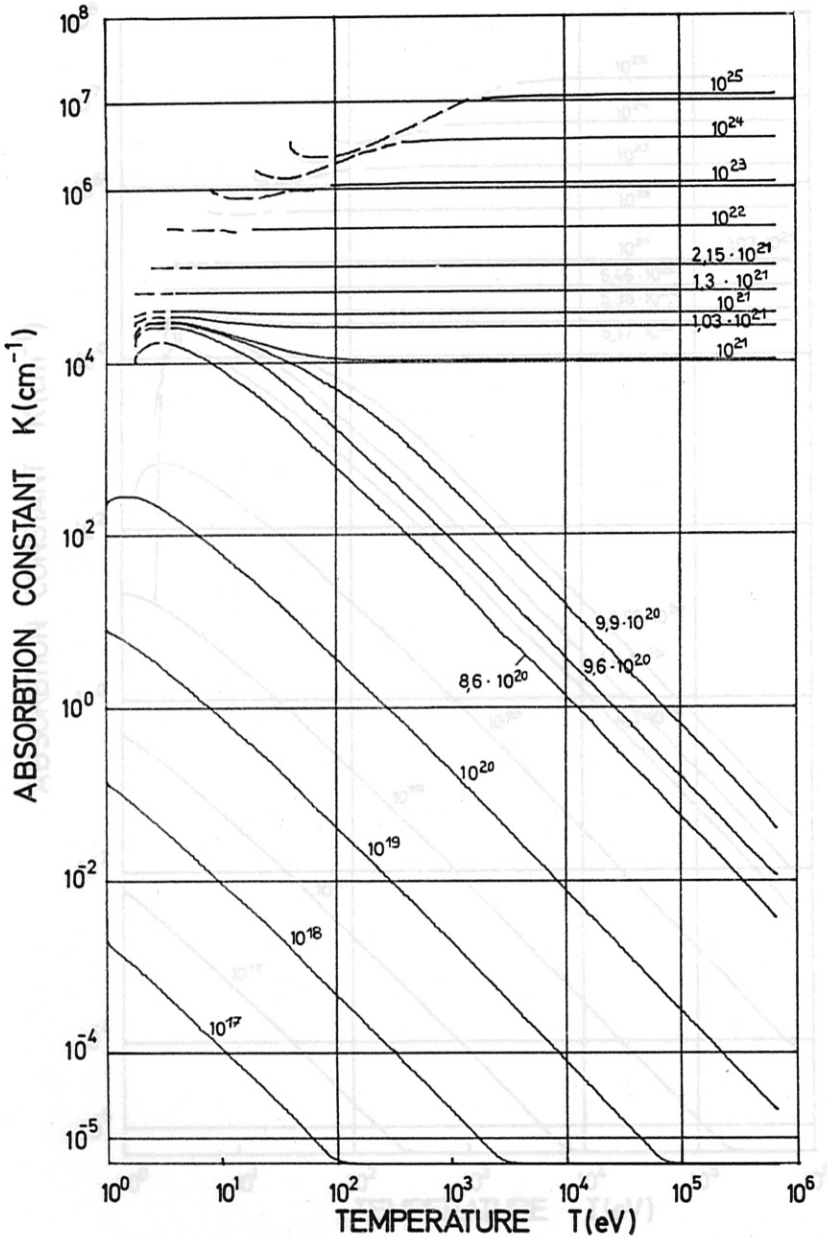

Fig. 9 Absorption constant K for neodymium glass laser radiation as a function of the electron temperature T and atomic densities N for full ionization with Z = 1 (hydrogen).

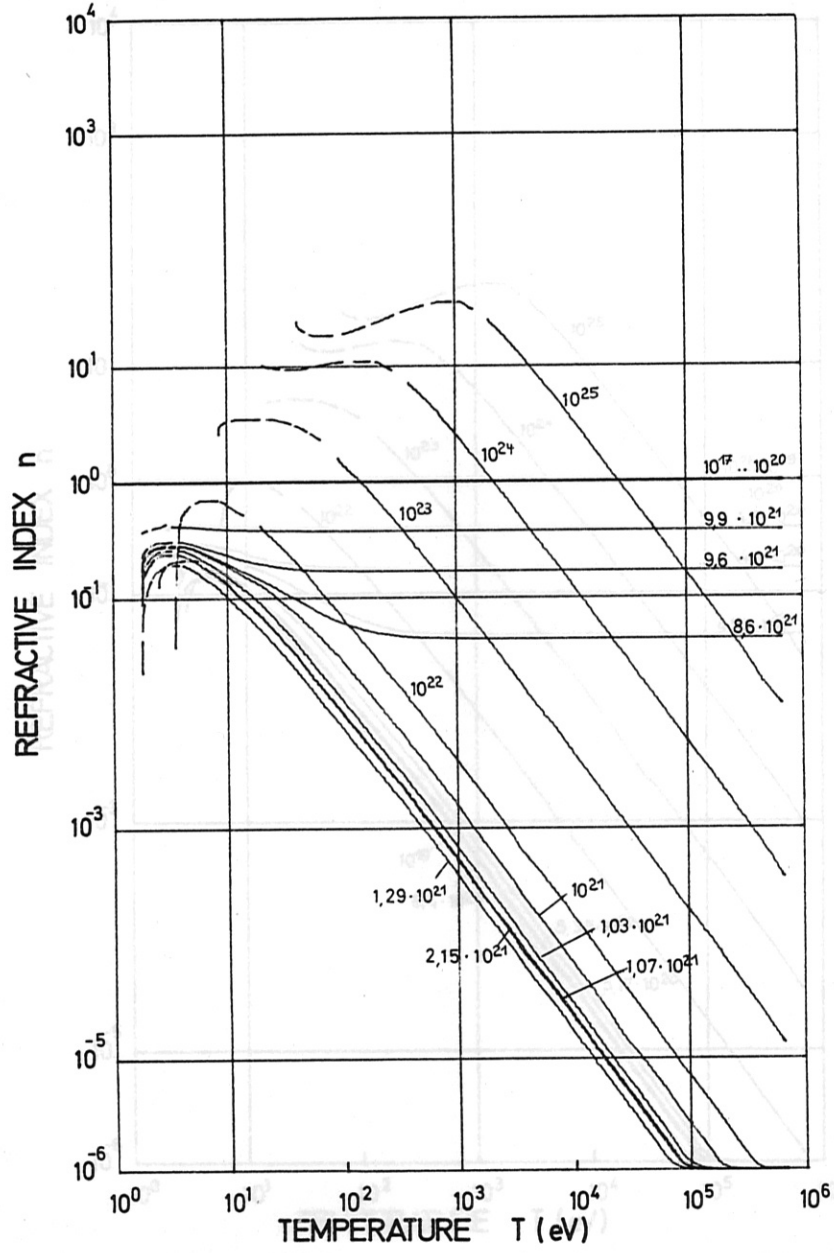

Fig. 10 Refractive index n for neodymium glass laser radiation as a function of the electron temperature T and atomic densities N for full ionization with Z = 1 (hydrogen).

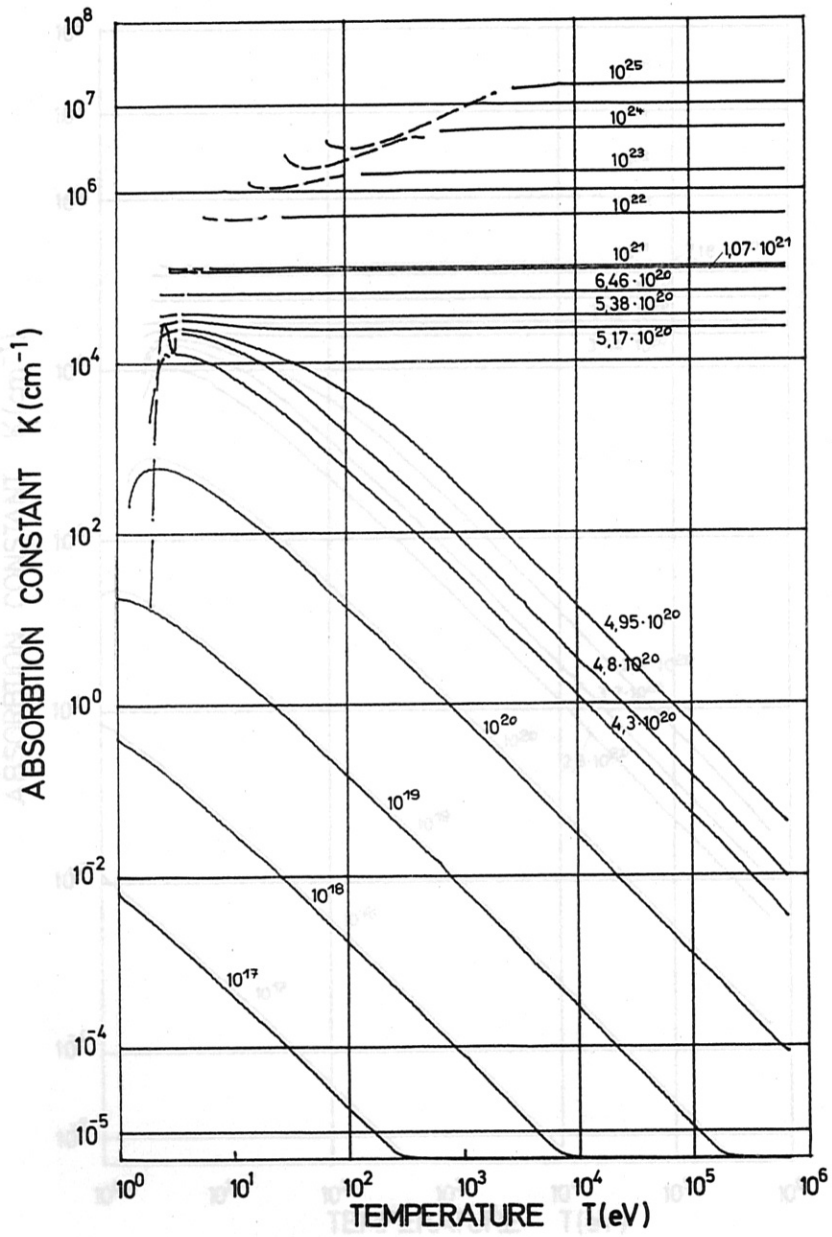

Fig. 11 Absorption constant K for neodymium glass laser radiation as a function of the electron temperature T and atomic densities N for full ionization with Z = 2 (helium).

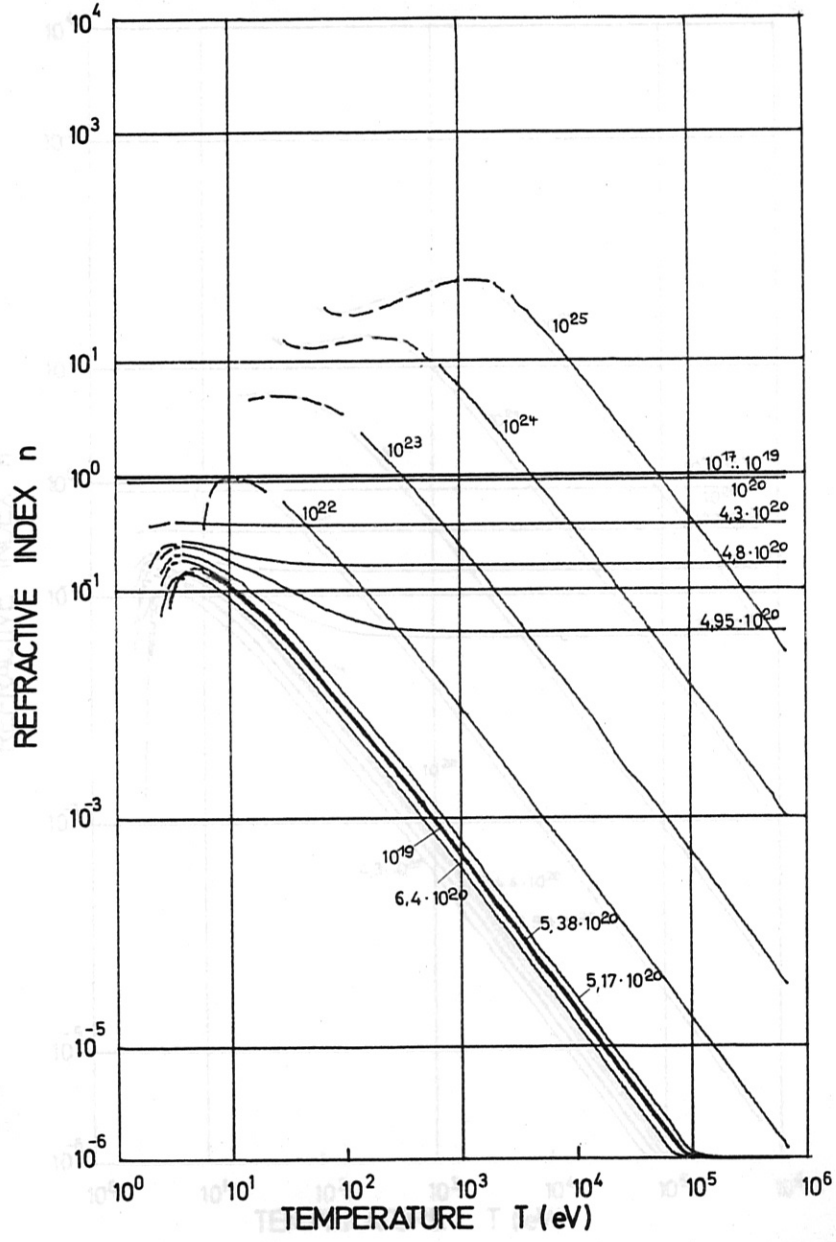

Fig. 12 Refractive index n for neodymium glass laser radiation as a function of the electron temperature T and atomic densities N for full ionization with Z = 2 (helium).

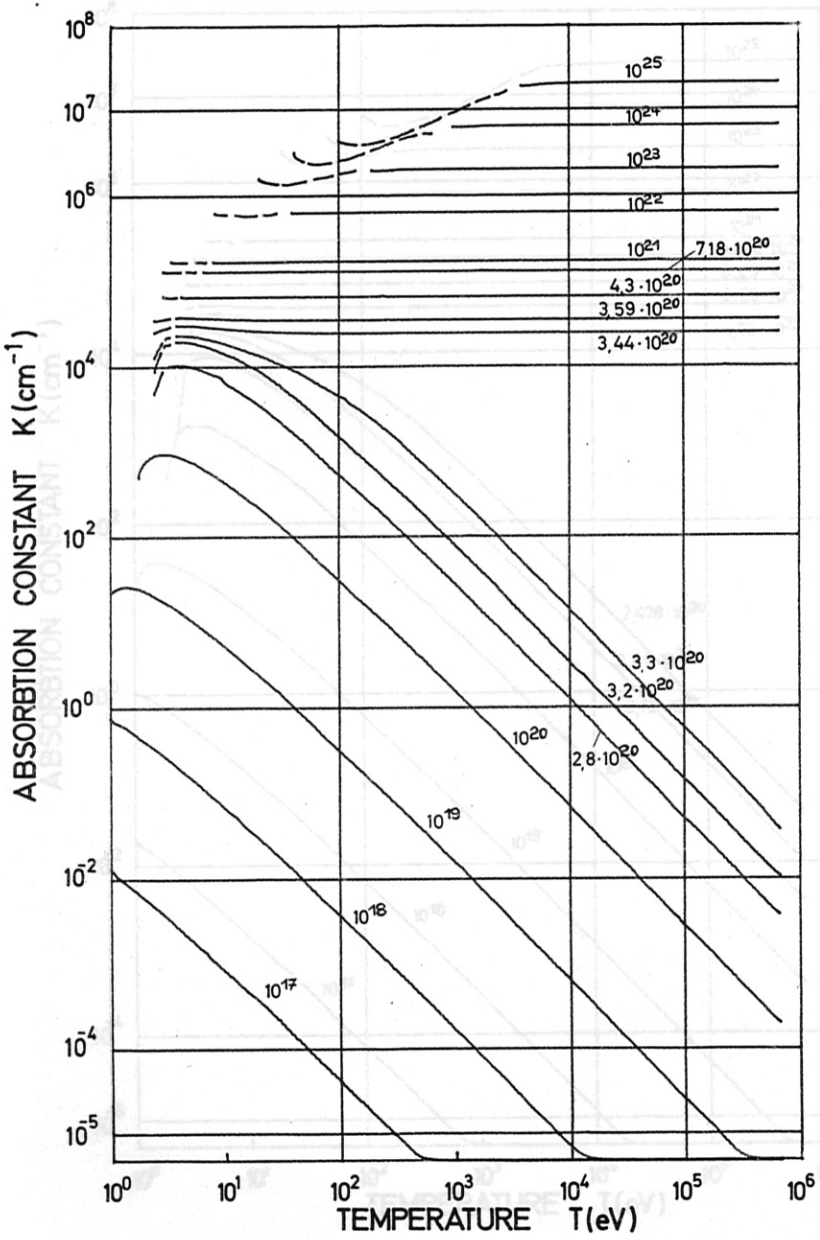

Fig. 13 Absorption constant K for neodymium glass laser radiation as a function of the electron temperature T and atomic densities N for full ionization with Z = 3 (lithium).

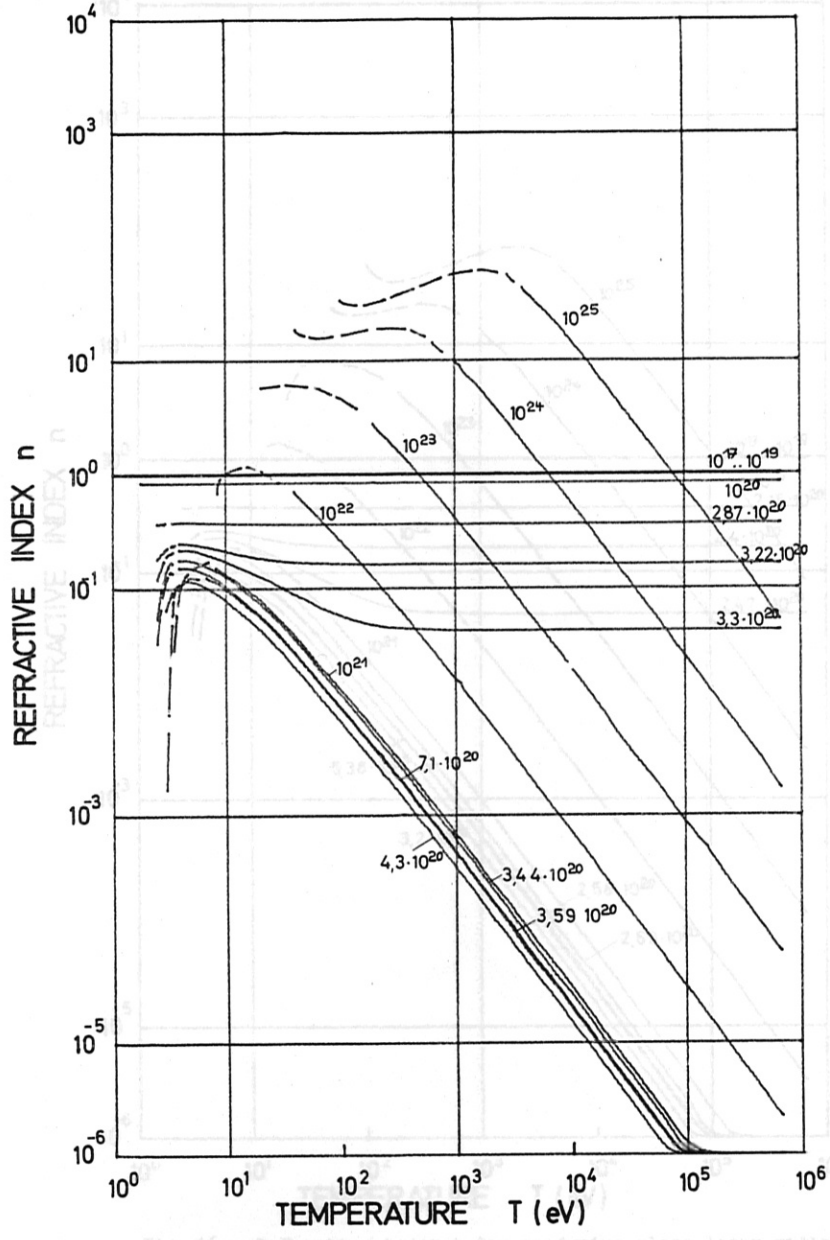

Fig. 14 Refractive index n for neodymium glass laser radiation as a function of the electron temperature T and atomic densities N for full ionization with Z = 3 (lithium).

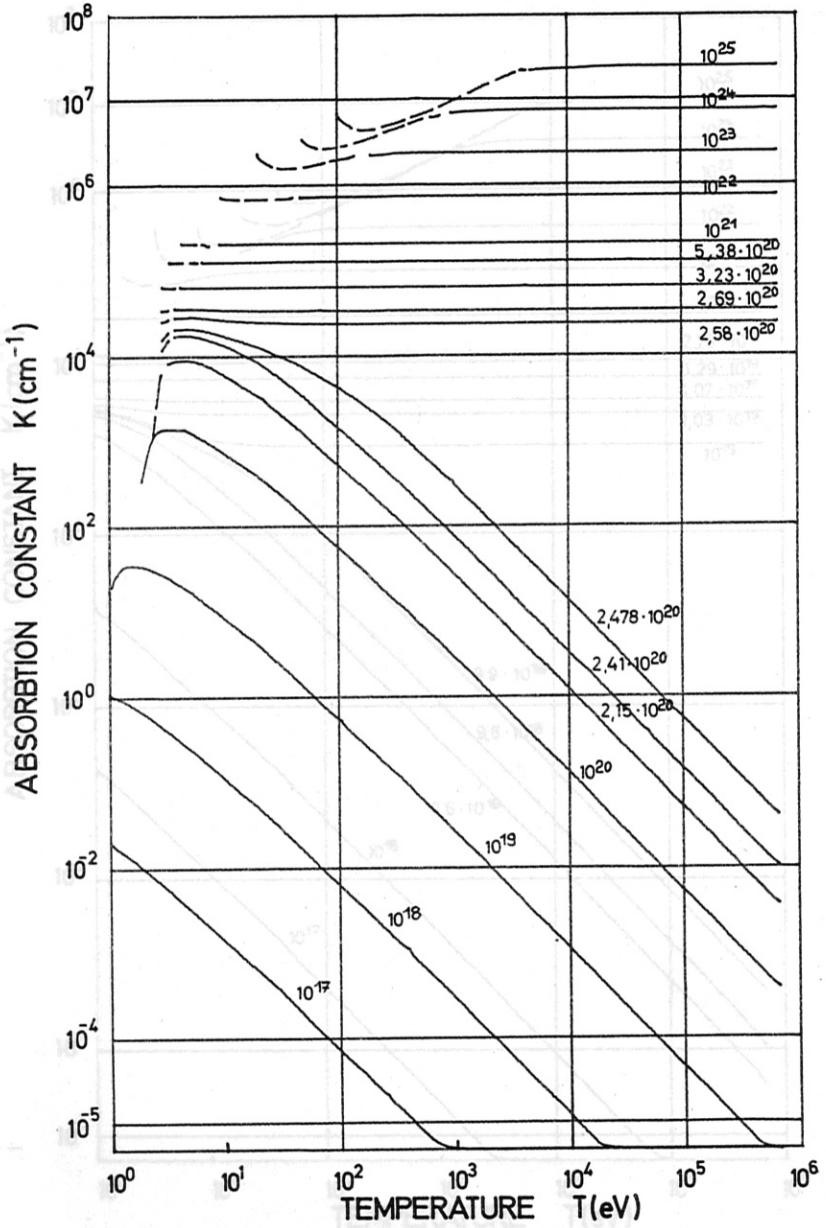

Fig. 15 Absorption constant K for neodymium glass laser radiation as a function of the electron temperature T and atomic densities N for full ionization with Z = 4 (beryllium).

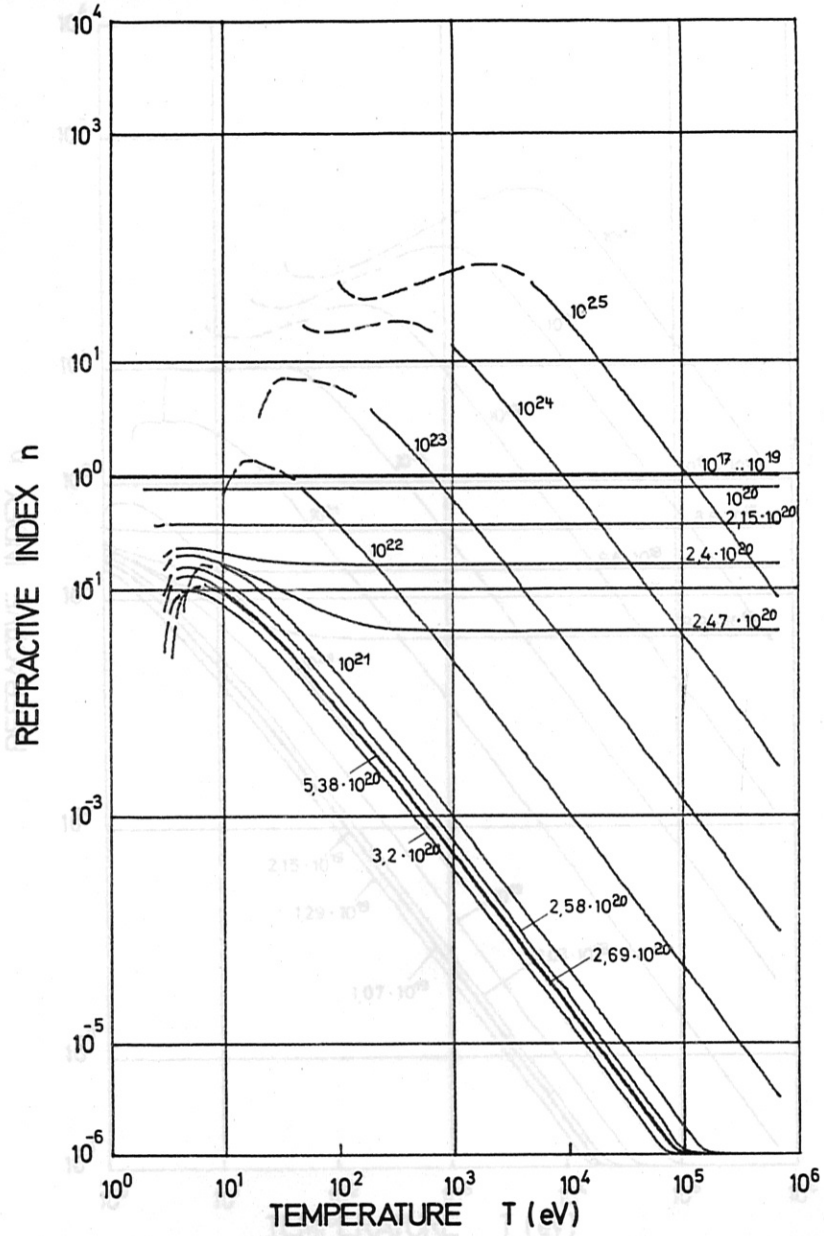

Fig. 16 Refractive index n for neodymium glass laser radiation as a function of the electron temperature T and atomic densities N for full ionization with Z = 4 (beryllium).

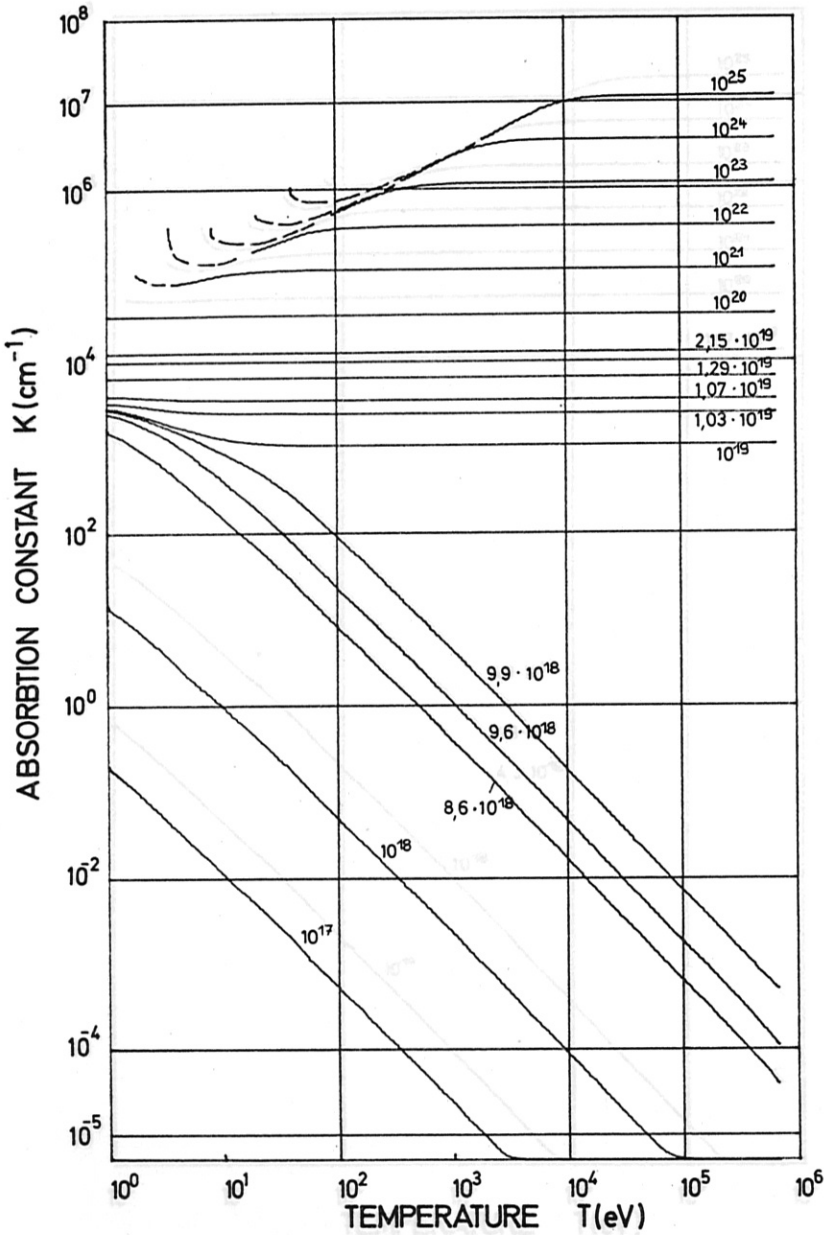

Fig. 17 Absorption constant K for CO_2-laser radiation as a function of the electron temperature T and atomic densities N for full ionization with Z = 1 (hydrogen).

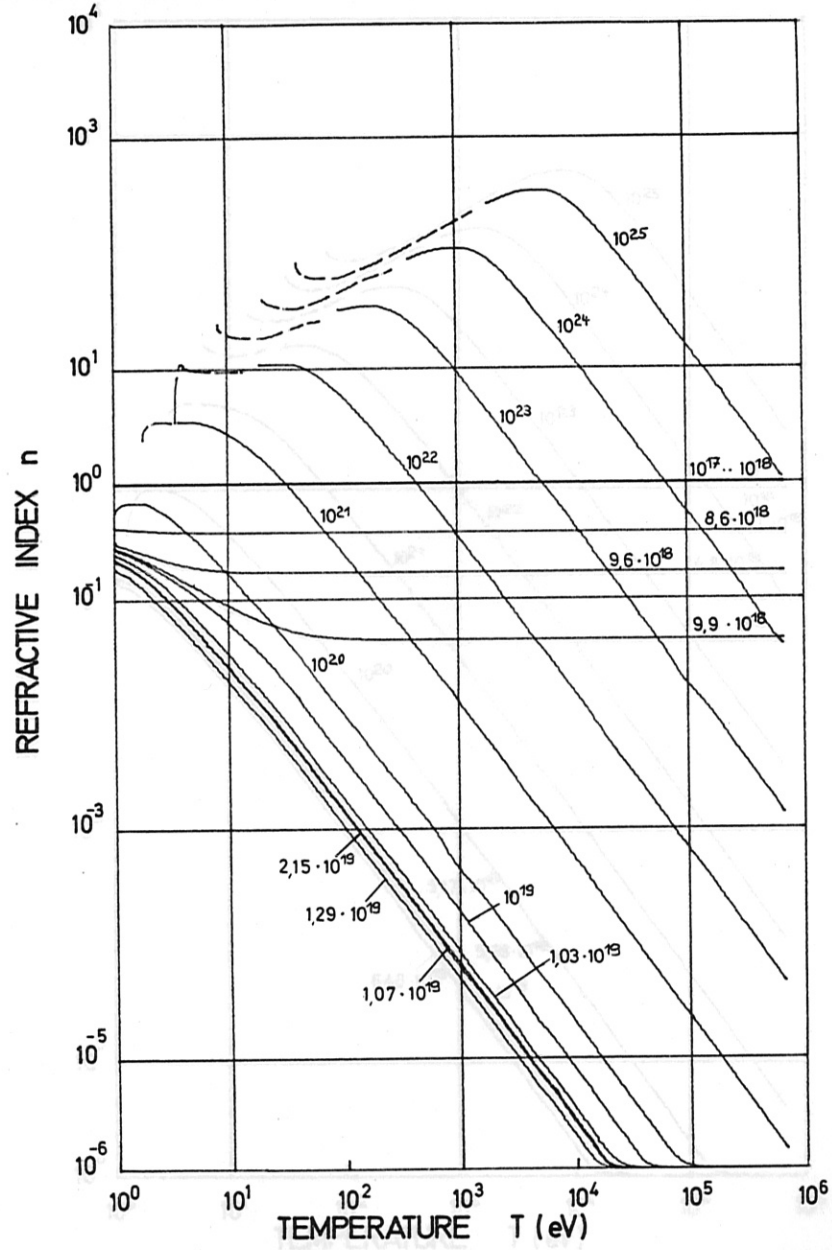

Fig. 18 Refractive index n for CO_2-laser radiation as a function of the electron temperature T and atomic densities N for full ionization with Z = 1 (hydrogen).

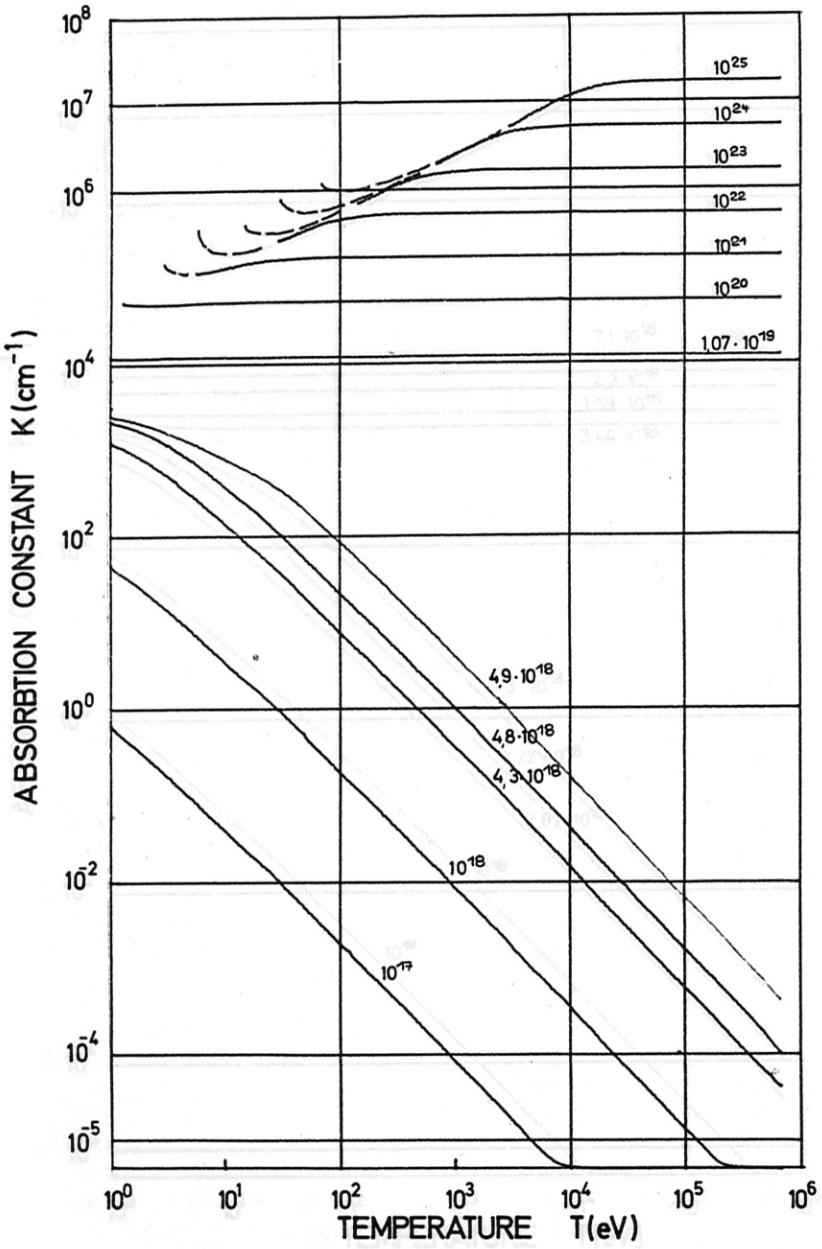

Fig. 19 Absorption constant K for CO_2-laser radiation as a function of the electron temperature T and atomic densities N for full ionization with Z = 2 (helium).

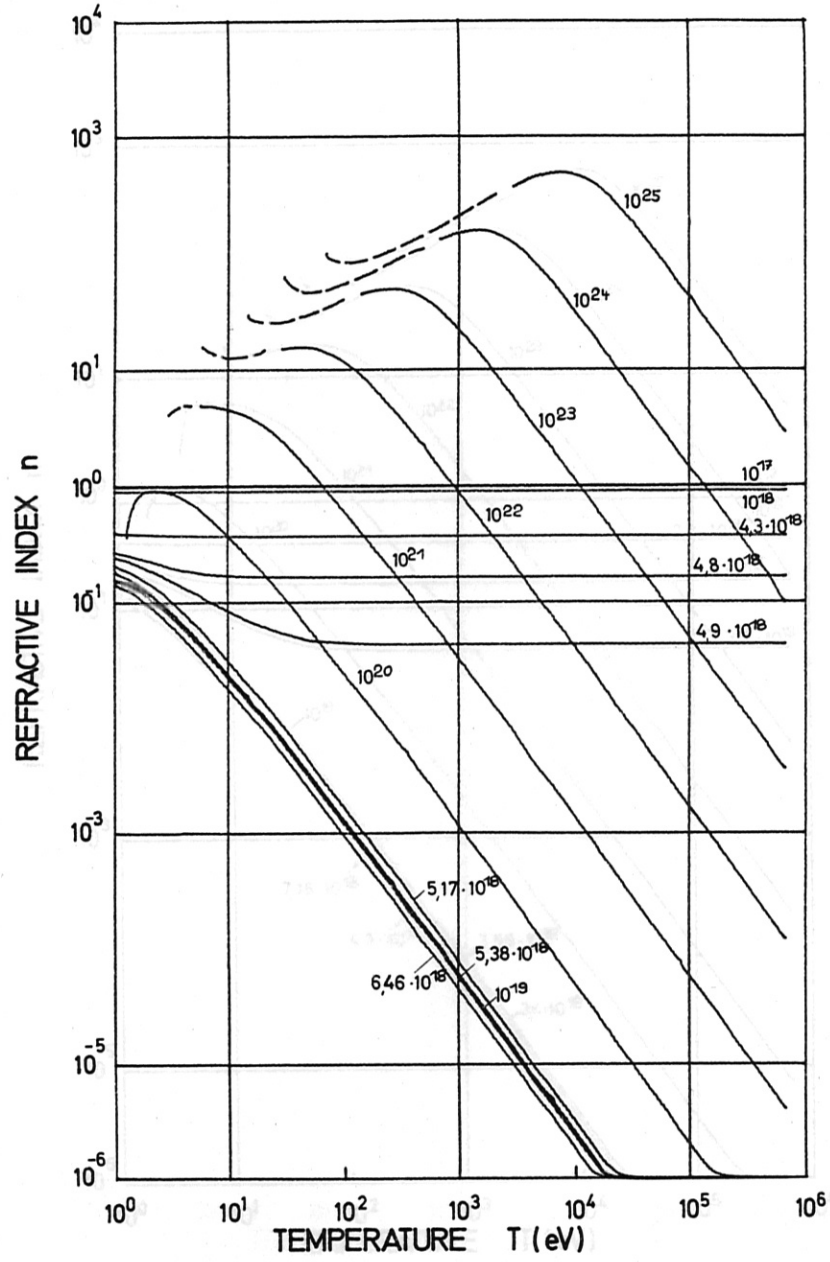

Fig. 20 Refractive index n for CO_2-laser radiation as a function of the electron temperature T and atomic densities N for full ionization with Z = 2 (helium).

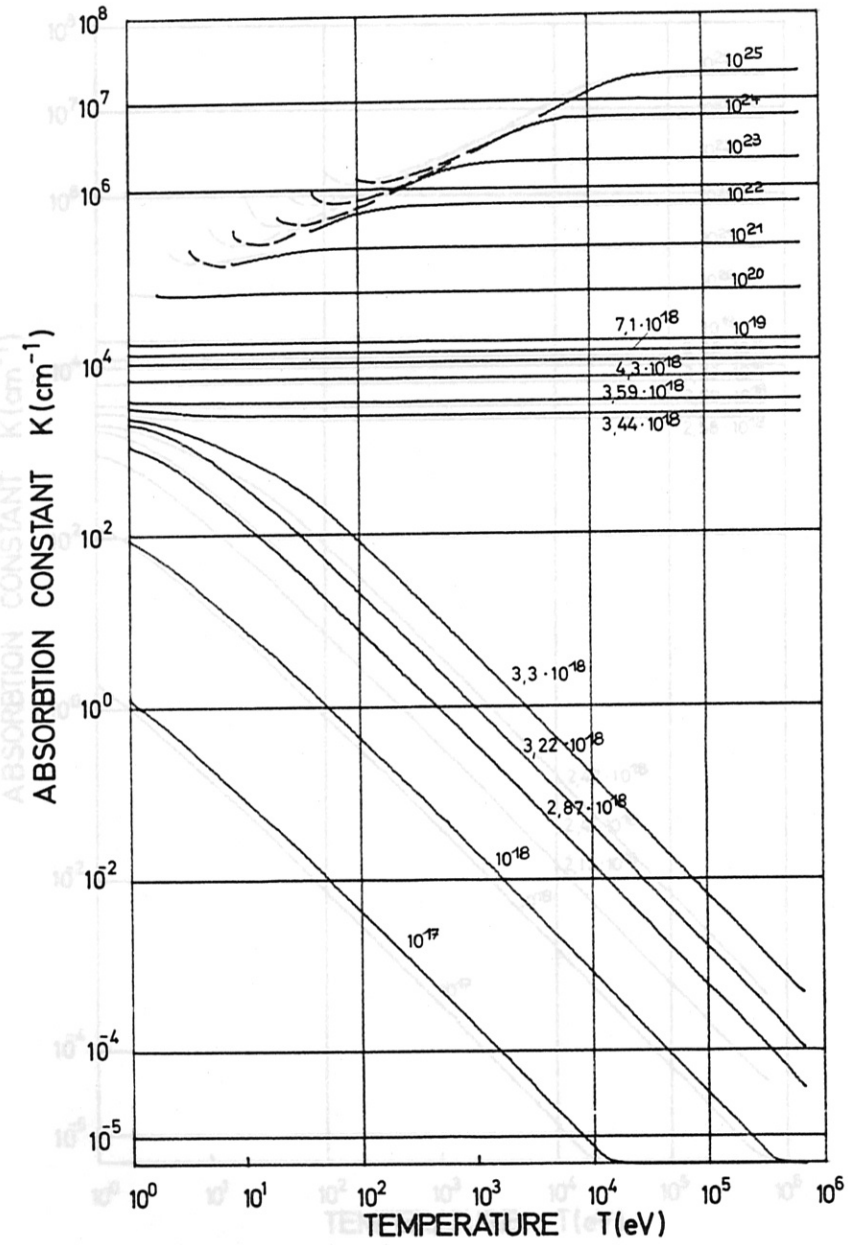

Fig. 21 Absorption constant K for CO_2-laser radiation as a function of the electron temperature T and atomic densities N for full ionization with Z = 3 (lithium).

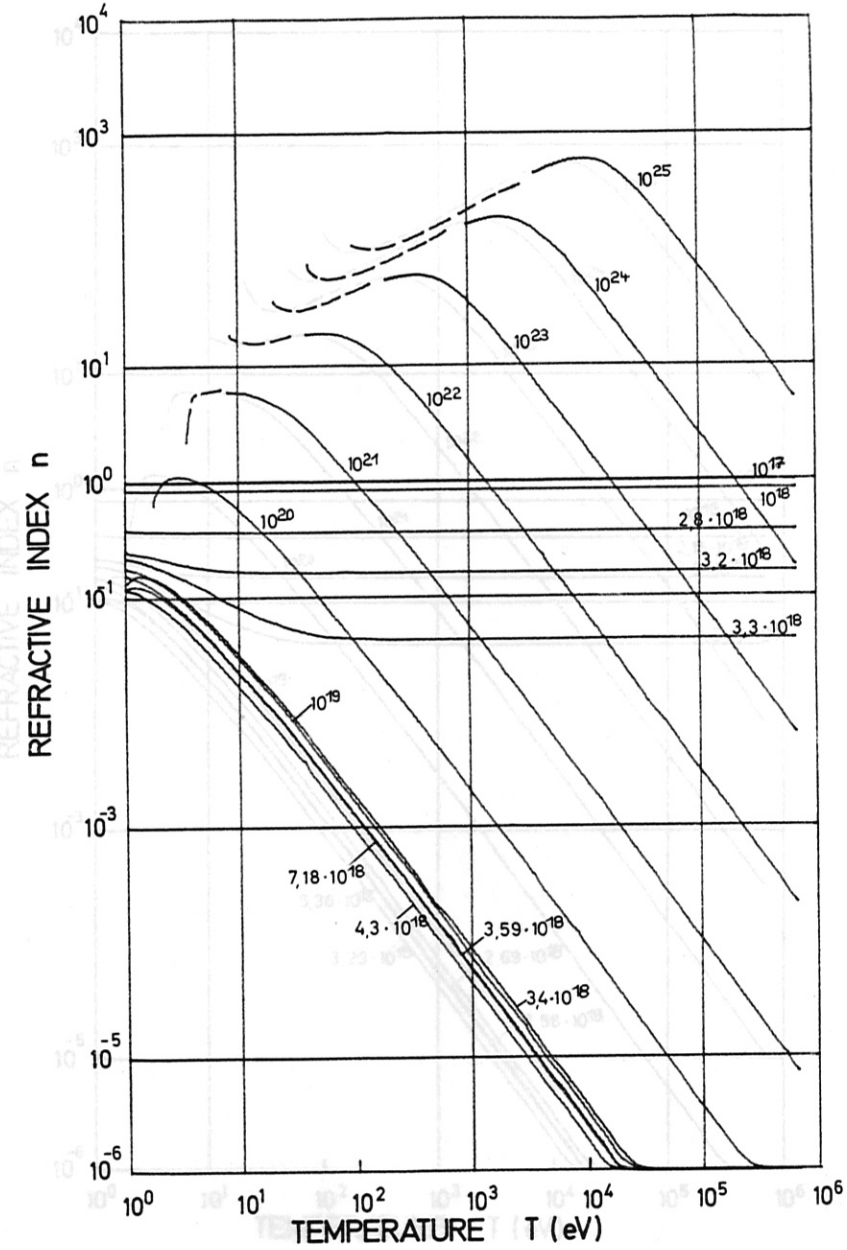

Fig. 22 Refractive index n for CO_2-laser radiation as a function of the electron temperature T and atomic densities N for full ionization with Z = 3 (lithium).

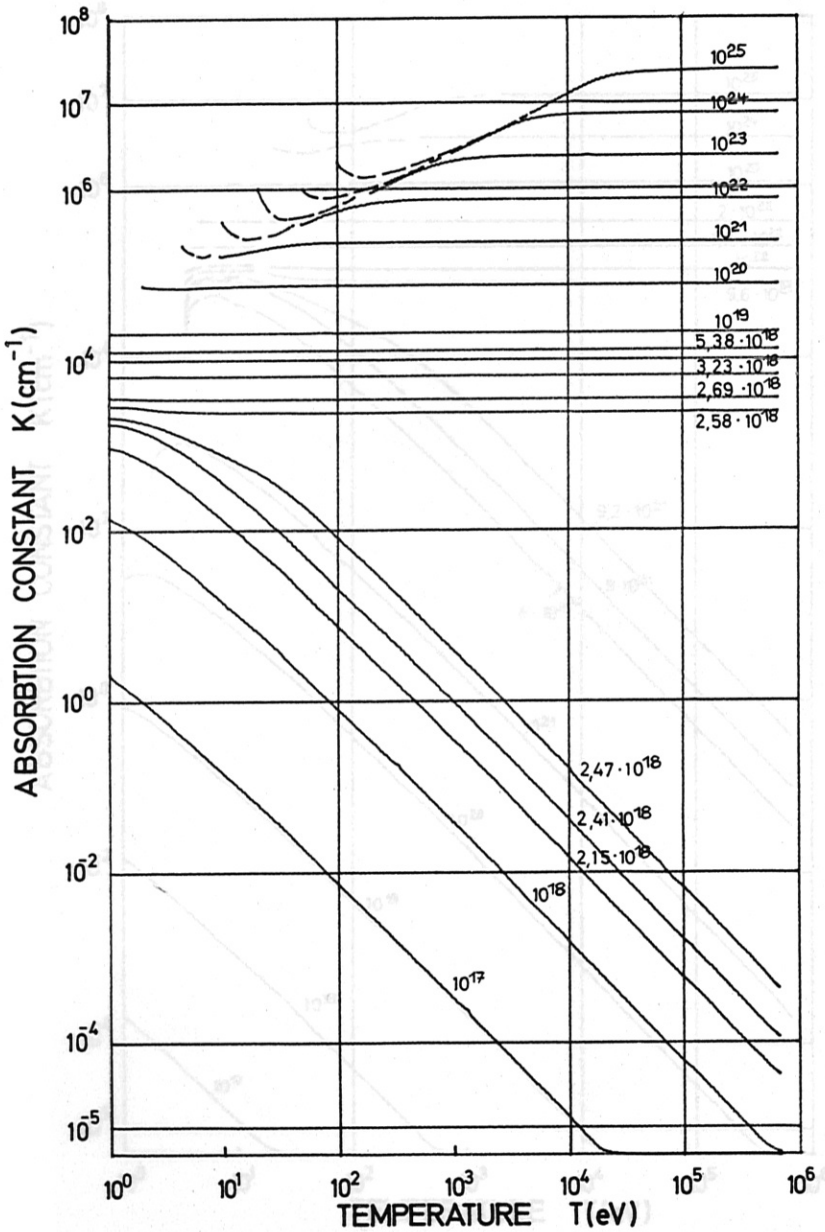

Fig. 23 Absorption constant K for CO_2-laser radiation as a function of the electron temperature T and atomic densities N for full ionization with Z = 4 (beryllium).

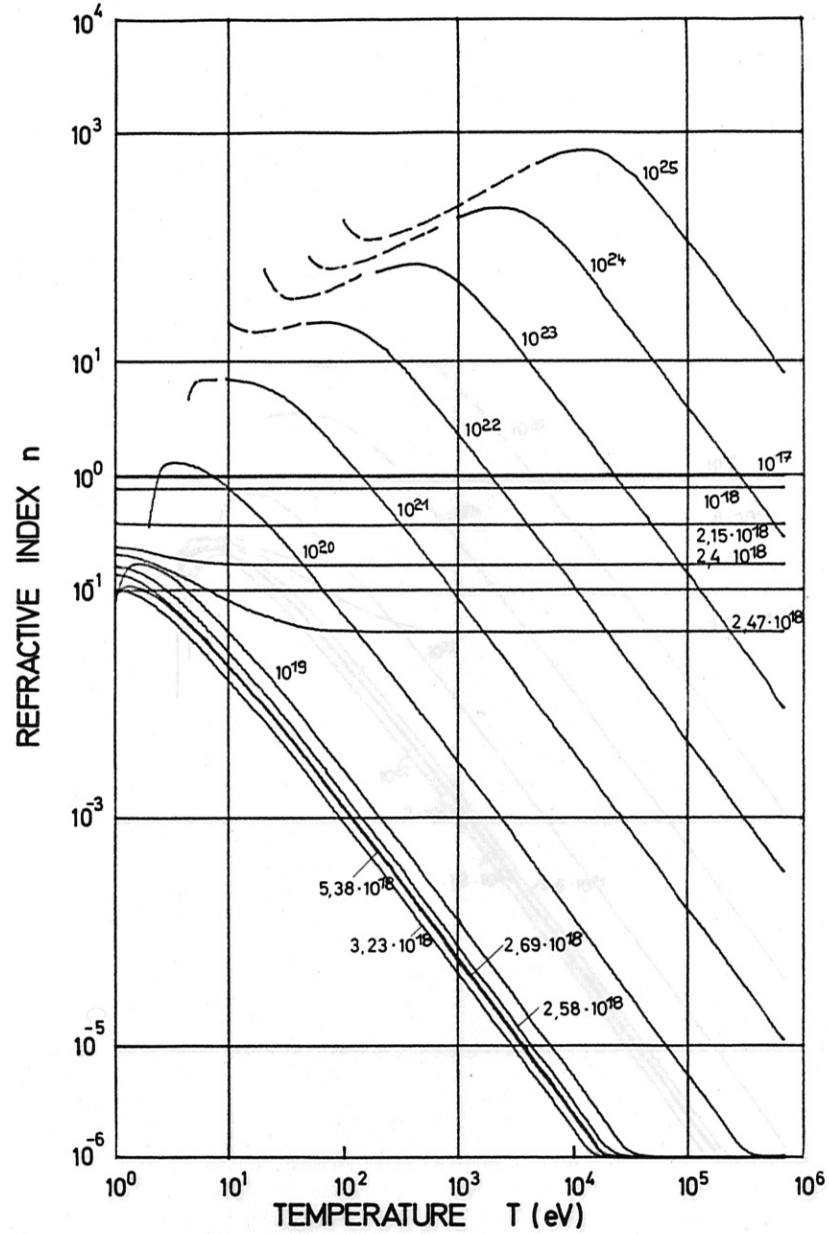

Fig. 24 Refractive index n for CO_2-laser radiation as a function of the electron temperature T and atomic densities N for full ionization with Z = 4 (beryllium).

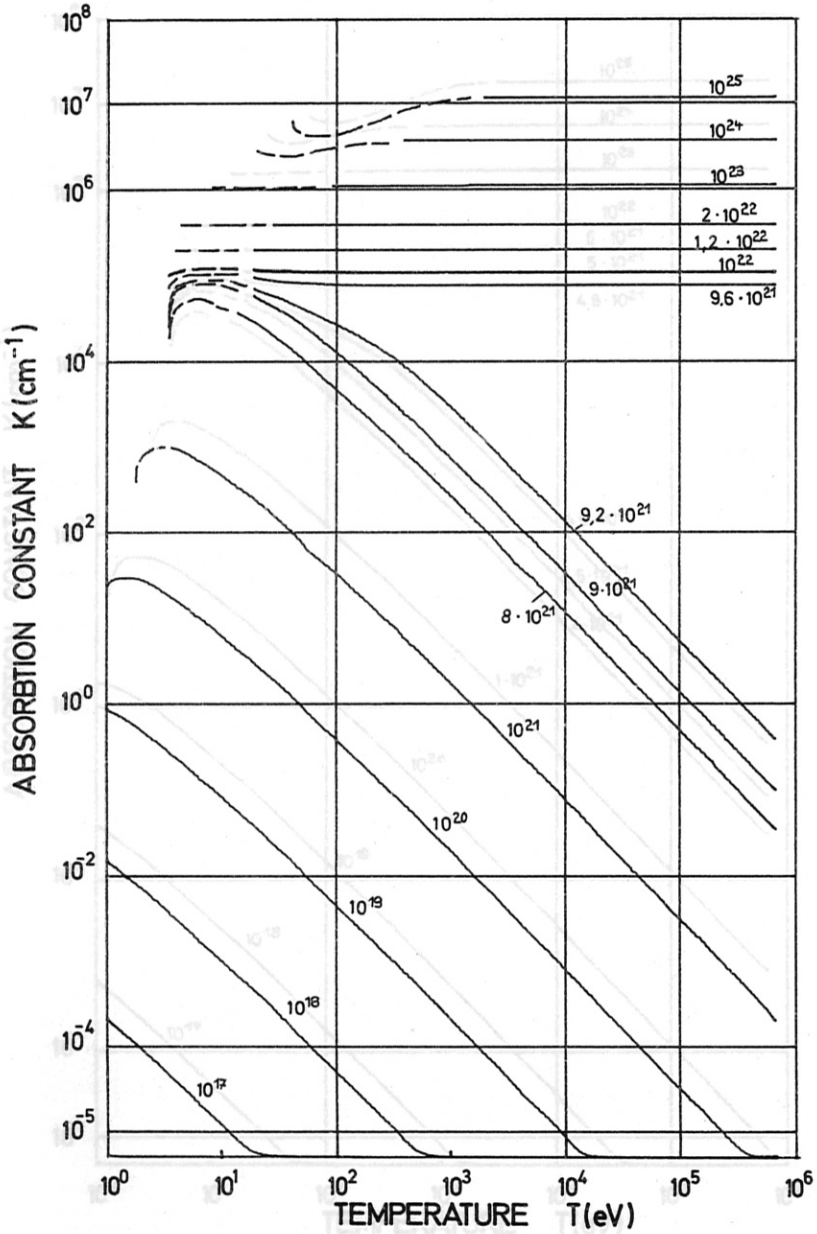

Fig. 25 Absorption constant K for the second harmonics of ruby laser radiation as a function of the electron temperature T and atomic densities N for full ionization with Z = 1 (hydrogen).

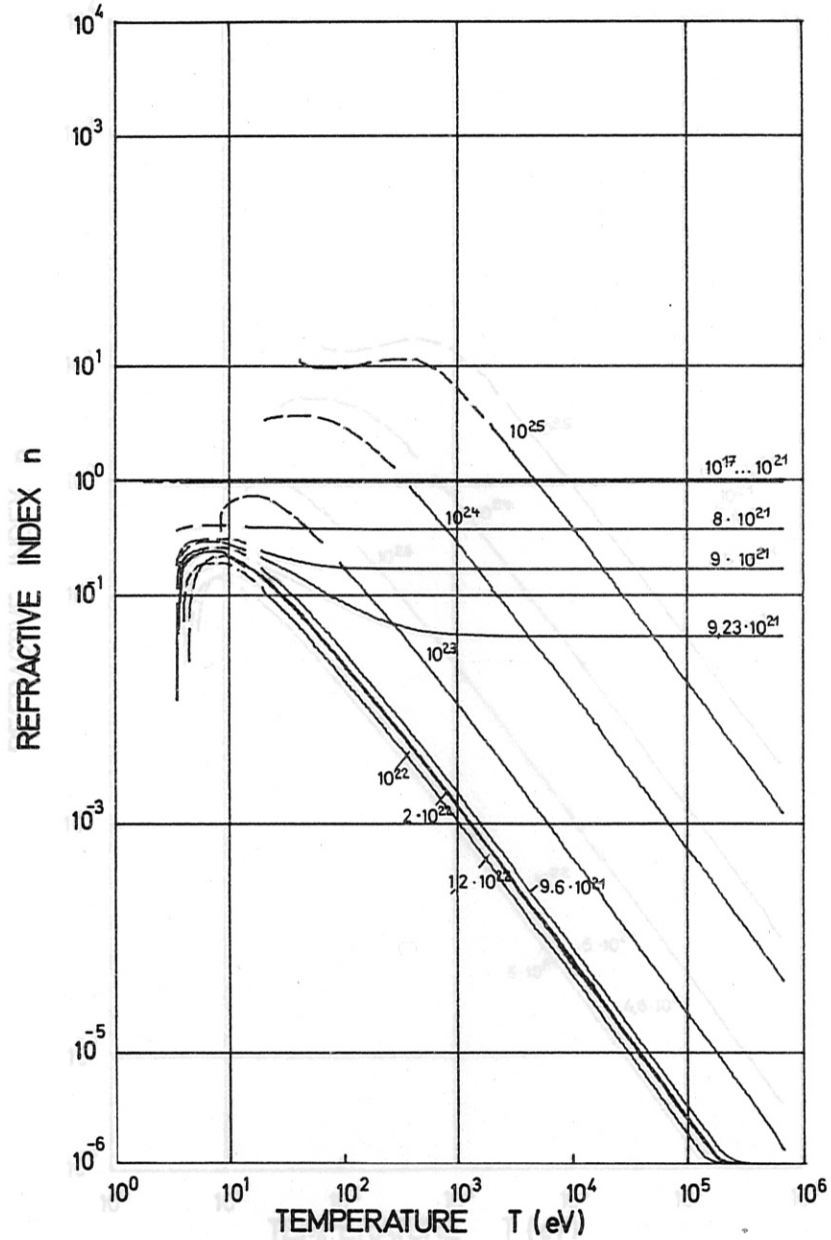

Fig. 26 Refractive index n for the second harmonics of ruby laser radiation as a function of the electron temperature T and atomic densities N for full ionization with Z = 1 (hydrogen).

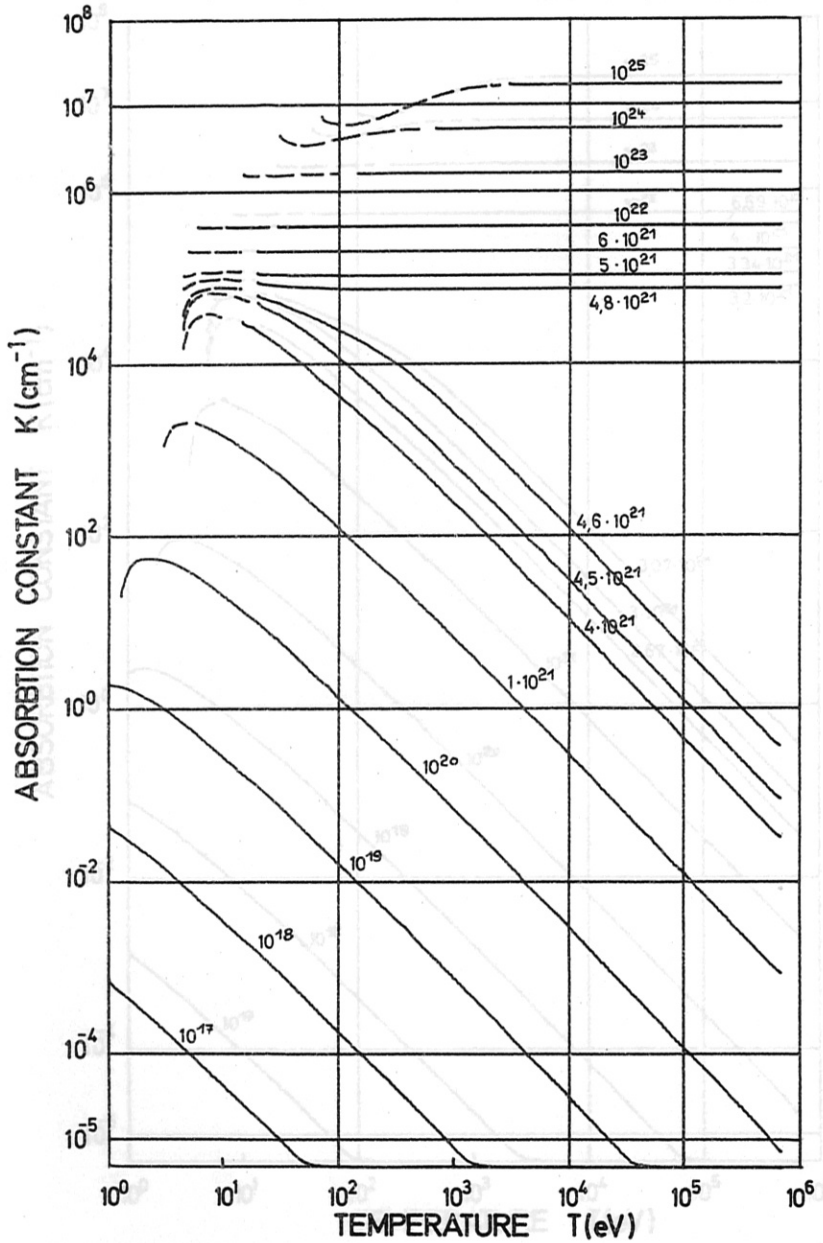

Fig. 27 Absorption constant K for the second harmonics of ruby laser radiation as a function of the electron temperature T and atomic densities N for full ionization with Z = 2 (helium).

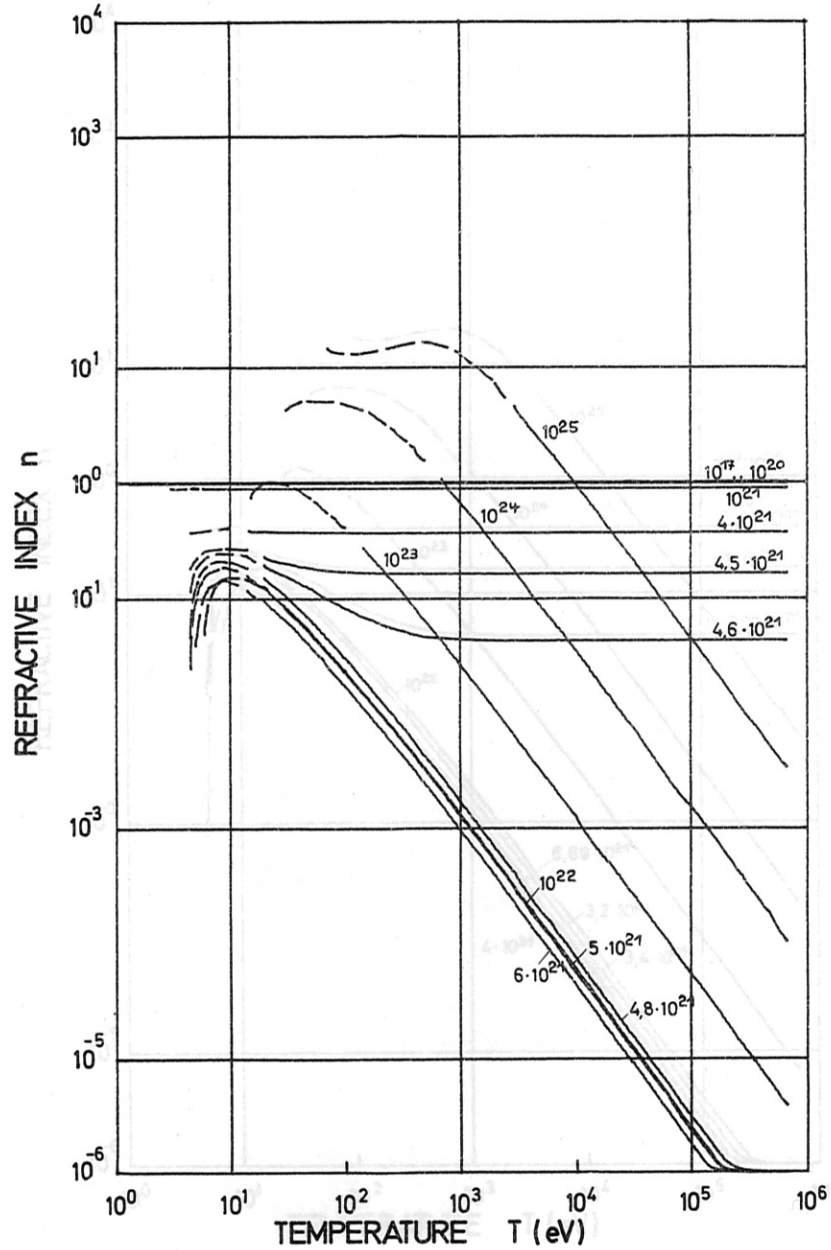

Fig. 28 Refractive index n for the second harmonics of ruby laser radiation as a function of the electron temperature T and atomic densities N for full ionization with Z = 2 (helium).

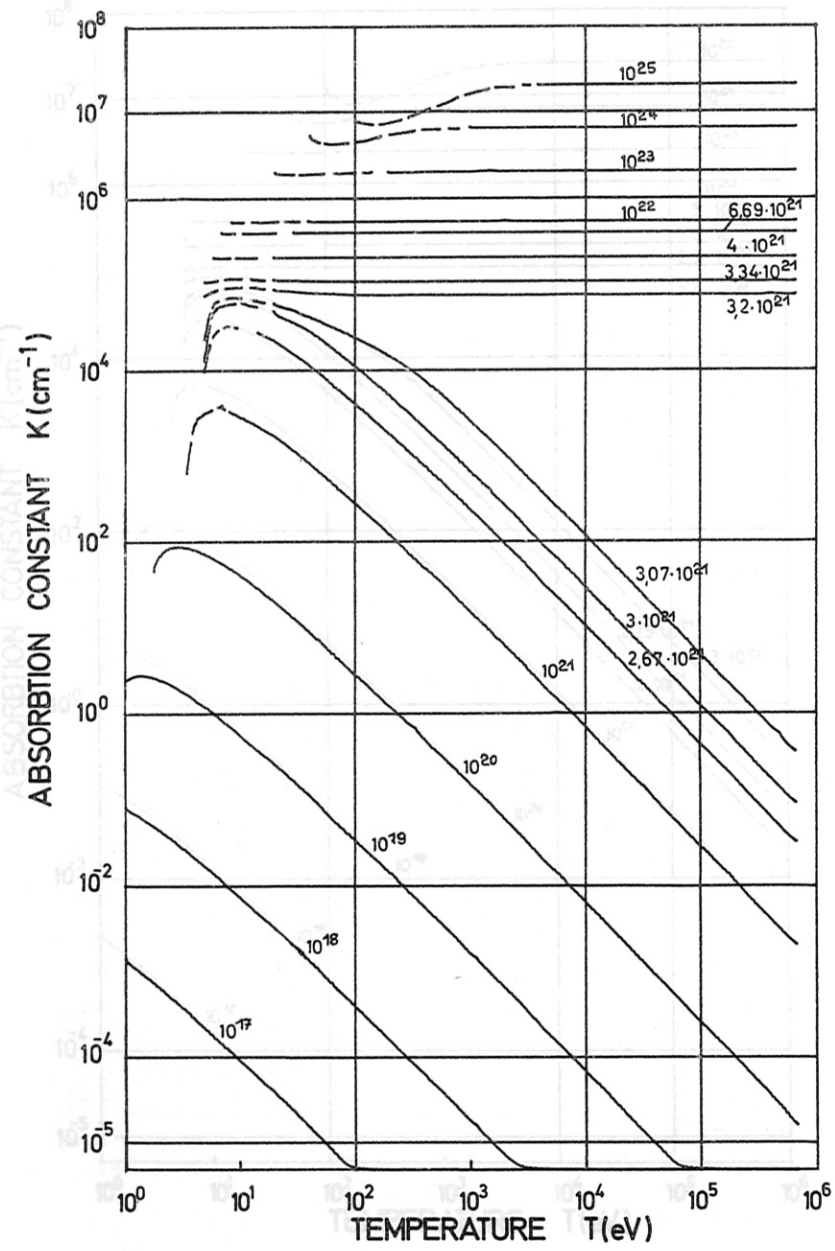

Fig. 29 Absorption constant K for the second harmonics of ruby laser radiation as a function of the electron temperature T and atomic densities N for full ionization with Z = 3 (lithium).

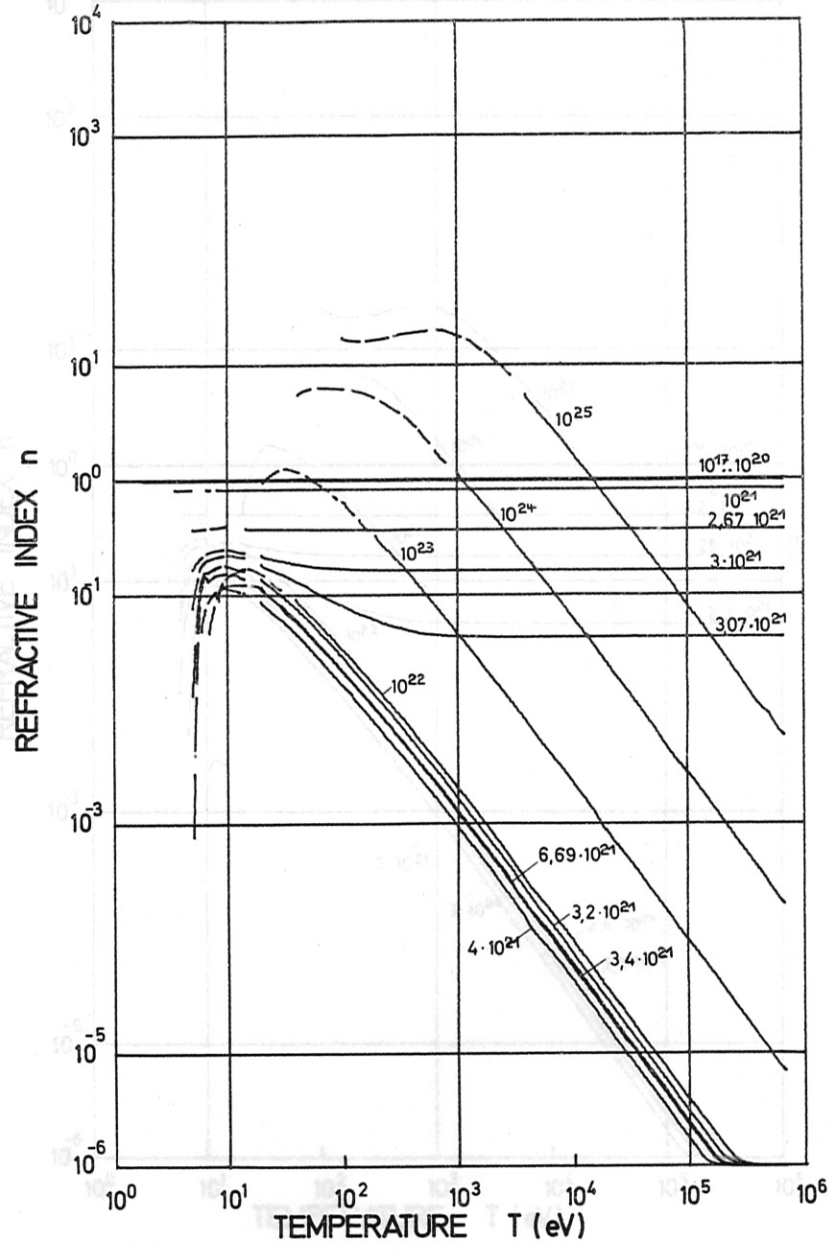

Fig. 30 Refractive index n for the second harmonics of ruby laser radiation as a function of the electron temperature T and atomic densities N for full ionization with Z = 3 (lithium).

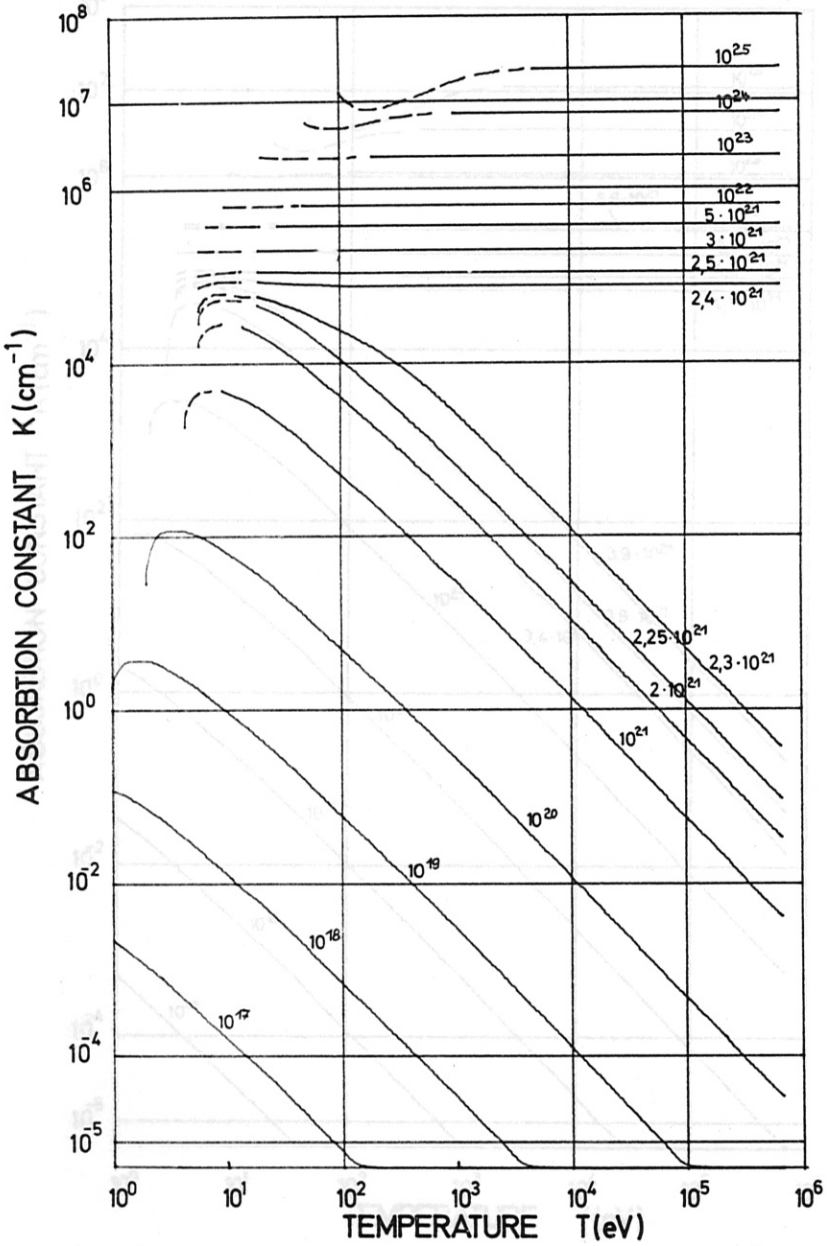

Fig. 31 Absorption constant K for the second harmonics of ruby laser radiation as a function of the electron temperatur T and atomic densities N for full ionization with Z = 4 (beryllium).

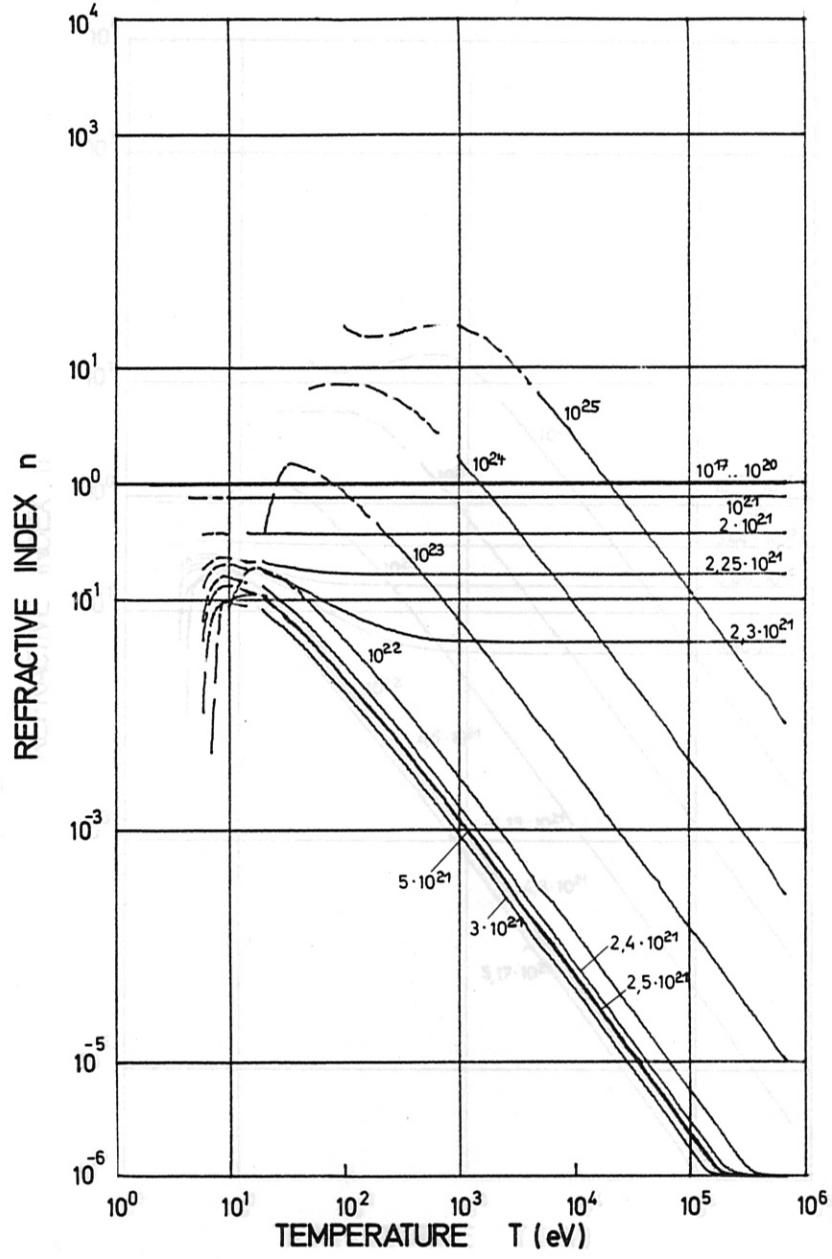

Fig. 32 Refractive index n for the second harmonics of ruby laser radiation as a function of the electron temperature T and atomic densities N for full ionization with Z = 4 (beryllium).

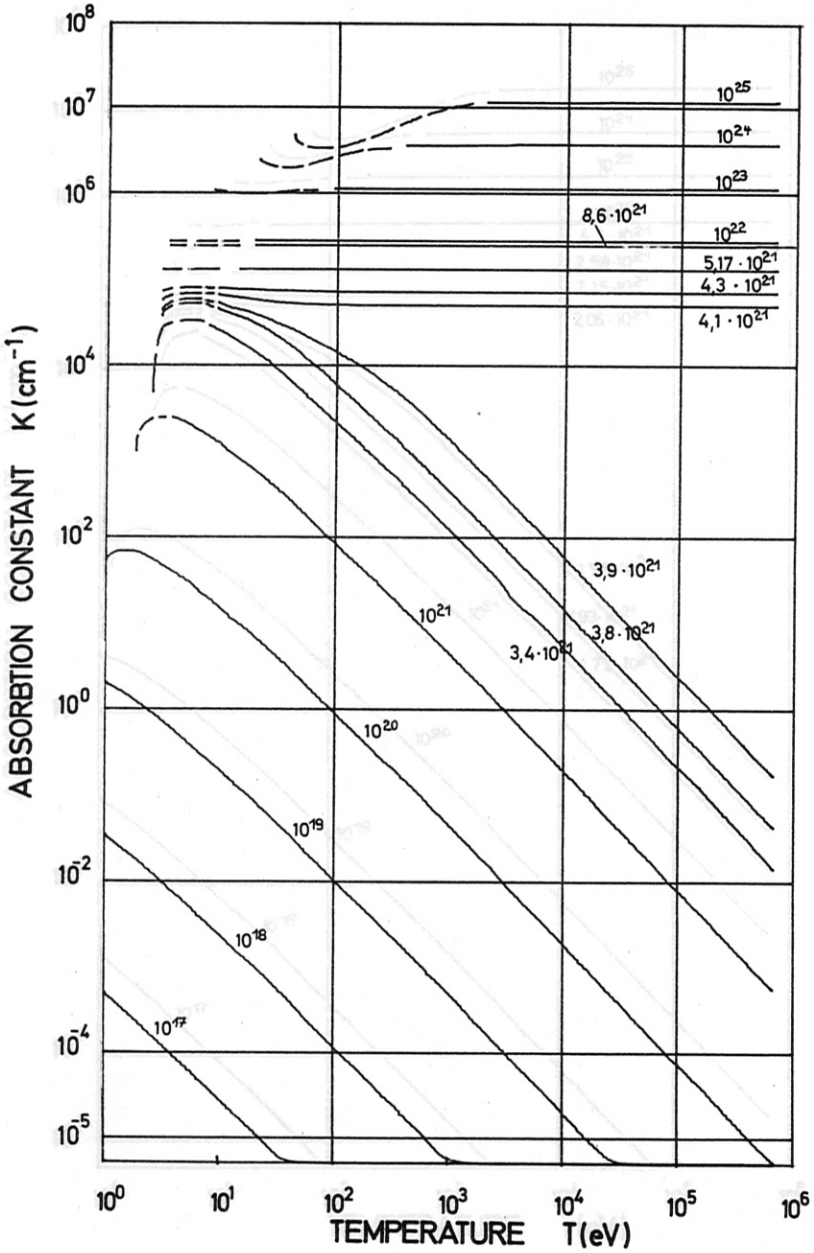

Fig. 33 Absorption constant K for the second harmonics of of neodymium glass laser radiation as a function of the electron temperature T and atomic densities N for full ionization with Z = 1 (hydrogen).

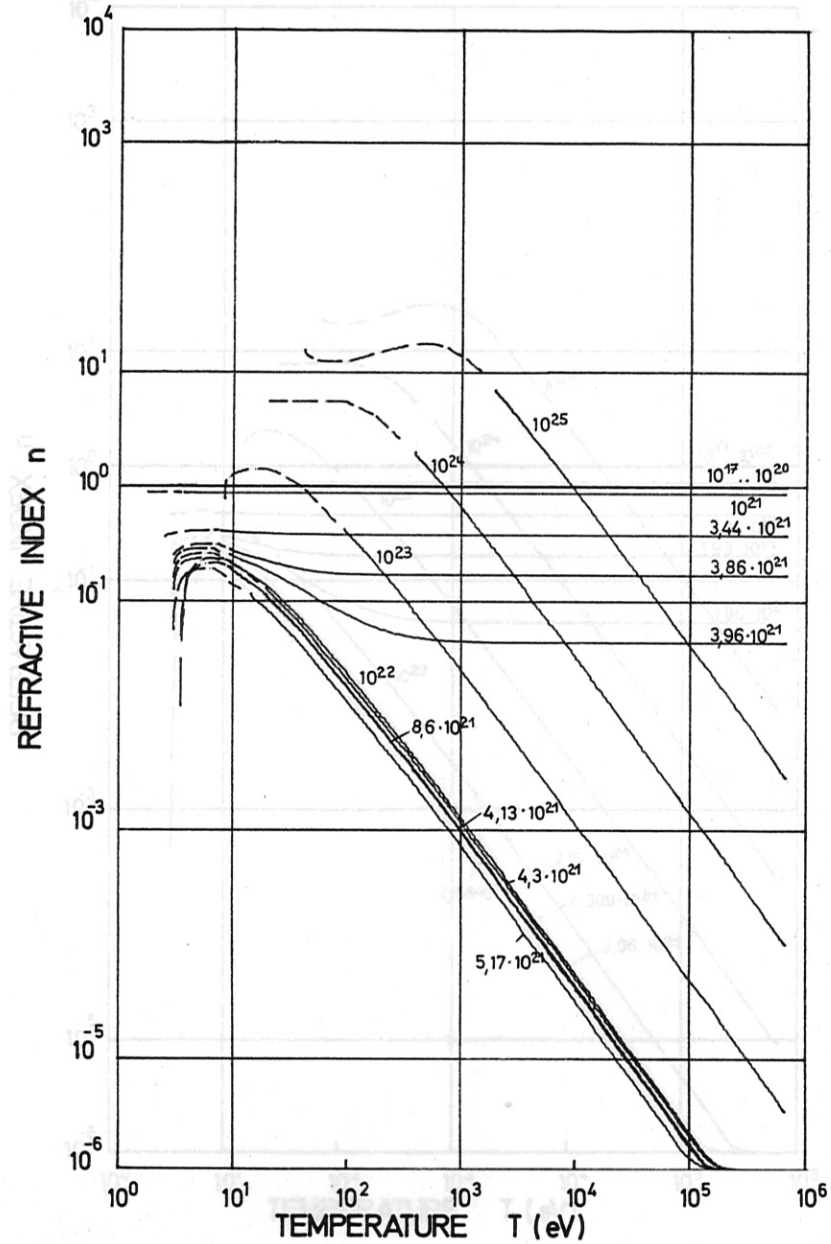

Fig. 34 Refractive index n for the second harmonics of neodymium glass laser radiation as a function of the electron temperature T and atomic densities N for full ionization with Z = 1 (hydrogen).

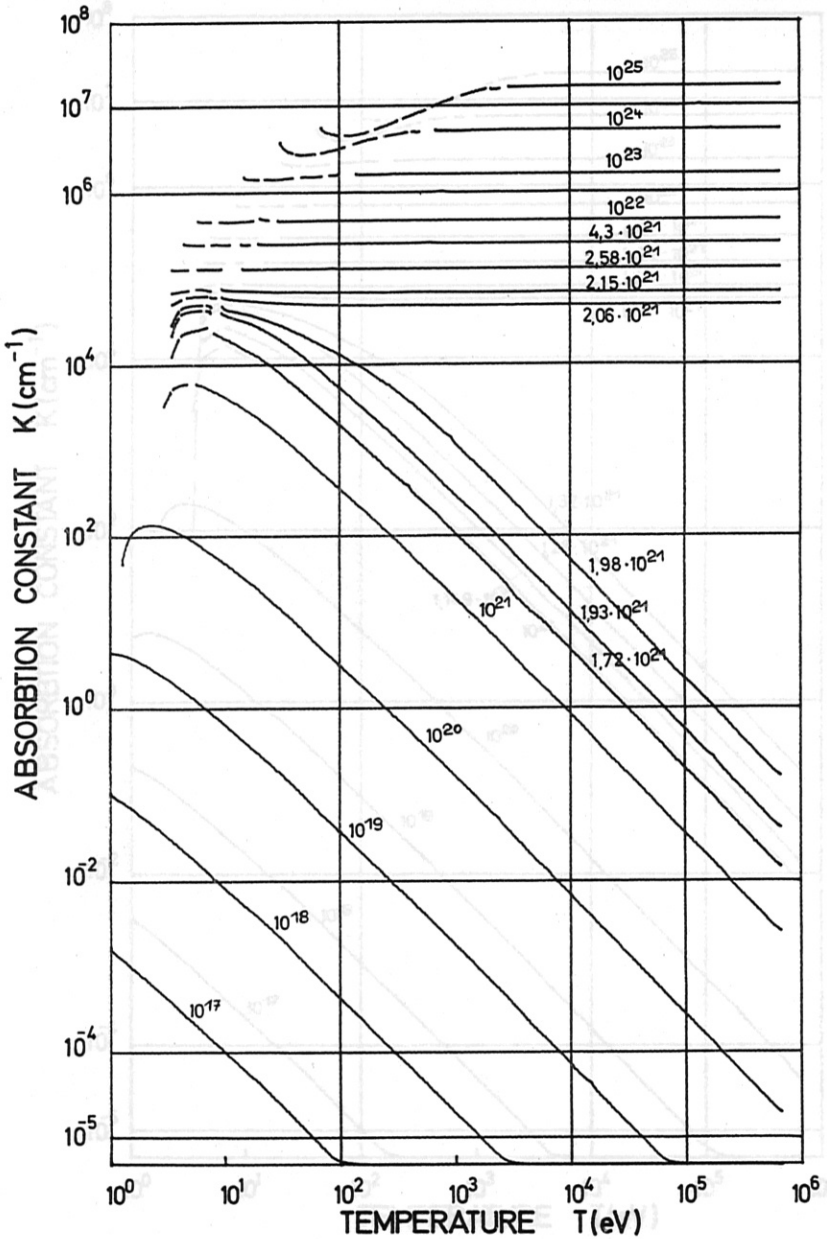

Fig. 35 Absorption constant K for the second harmonics of neodymium glass laser radiation as a function of the electron temperature T and atomic densities N for full ionization with Z = 2 (helium).

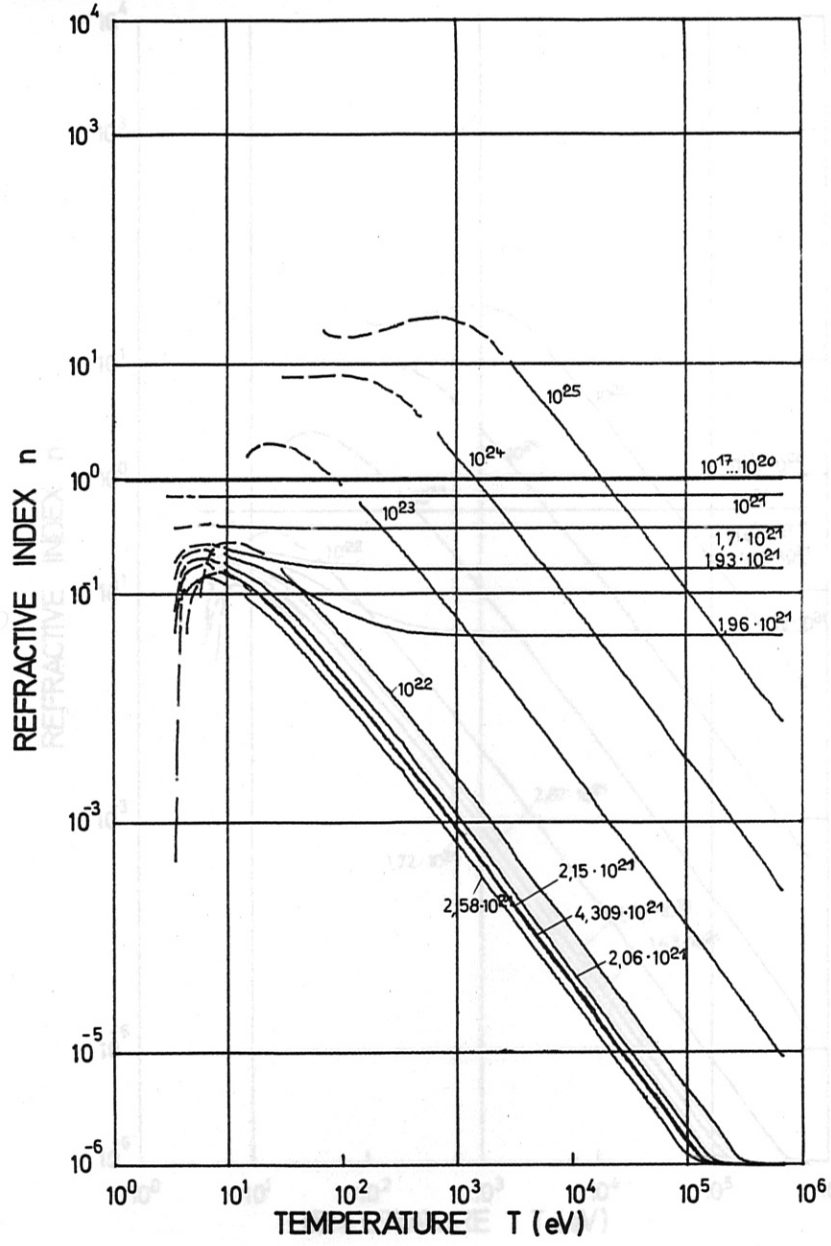

Fig. 36 Refractive index n for the second harmonics of neodymium glass laser radiation as a function of the electron temperature T and atomic densities N for full ionization with Z = 2 (helium).

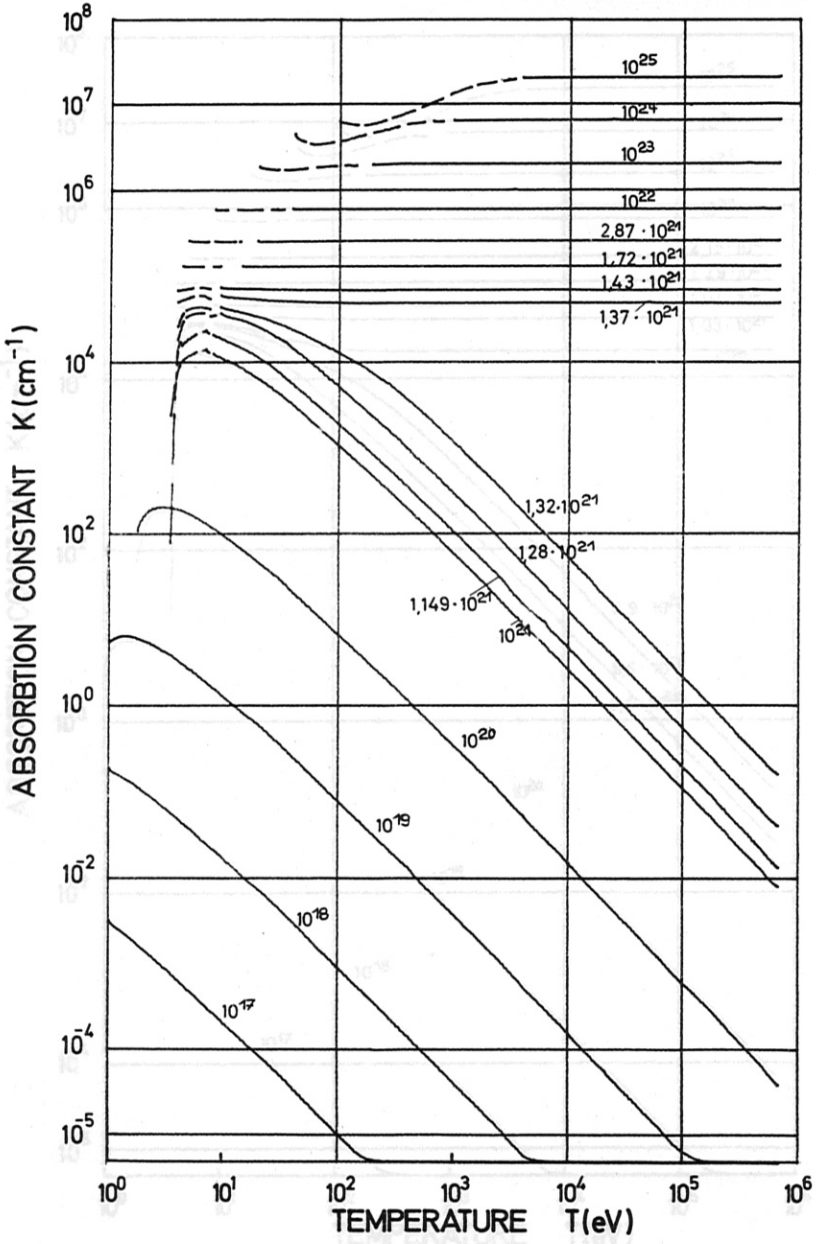

Fig. 37 Absorption constant K for the second harmonics of neodymium glass laser radiation as a function of the electron temperature T and atomic densities N for full ionization with Z = 3 (lithium).

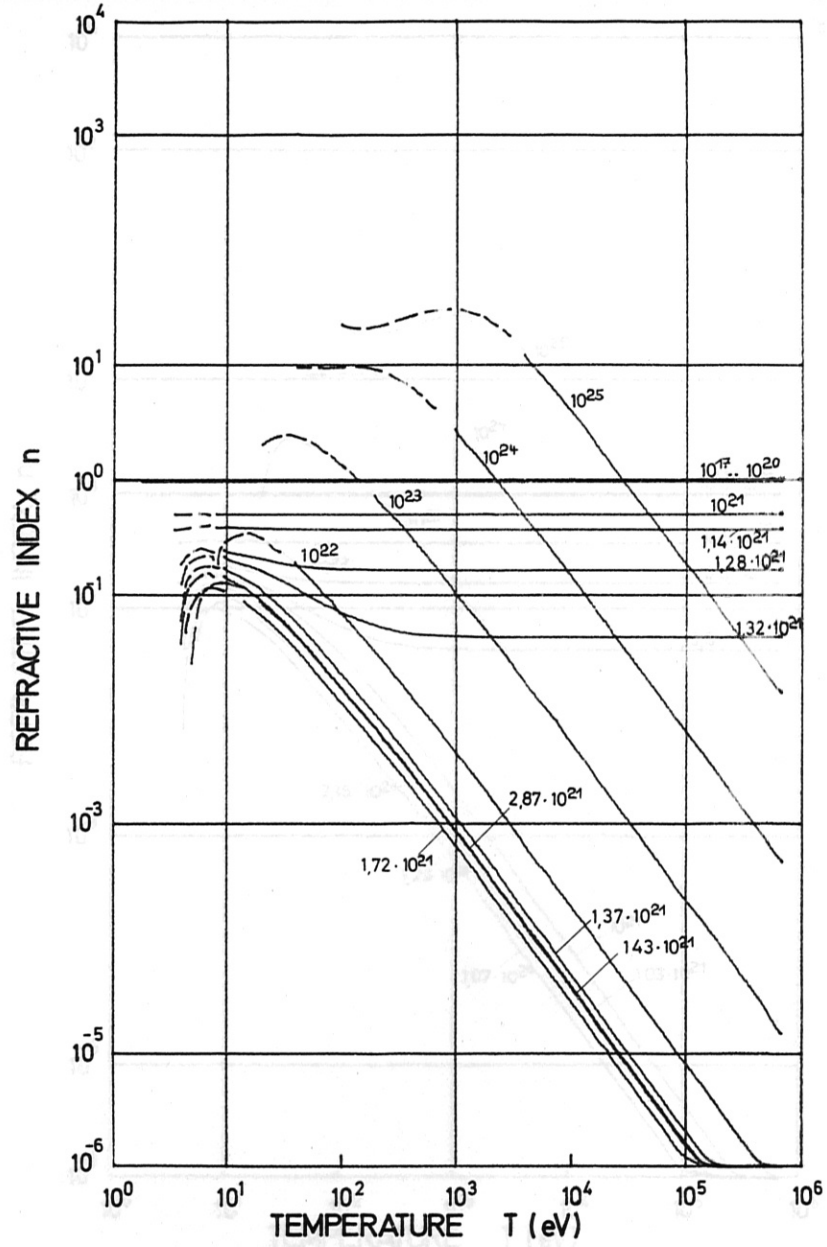

Fig. 38 Refractive index n for the second harmonics of neodymium glass laser radiation as a function of the electron temperature T and atomic densities N for full ionization with Z = 3 (lithium).

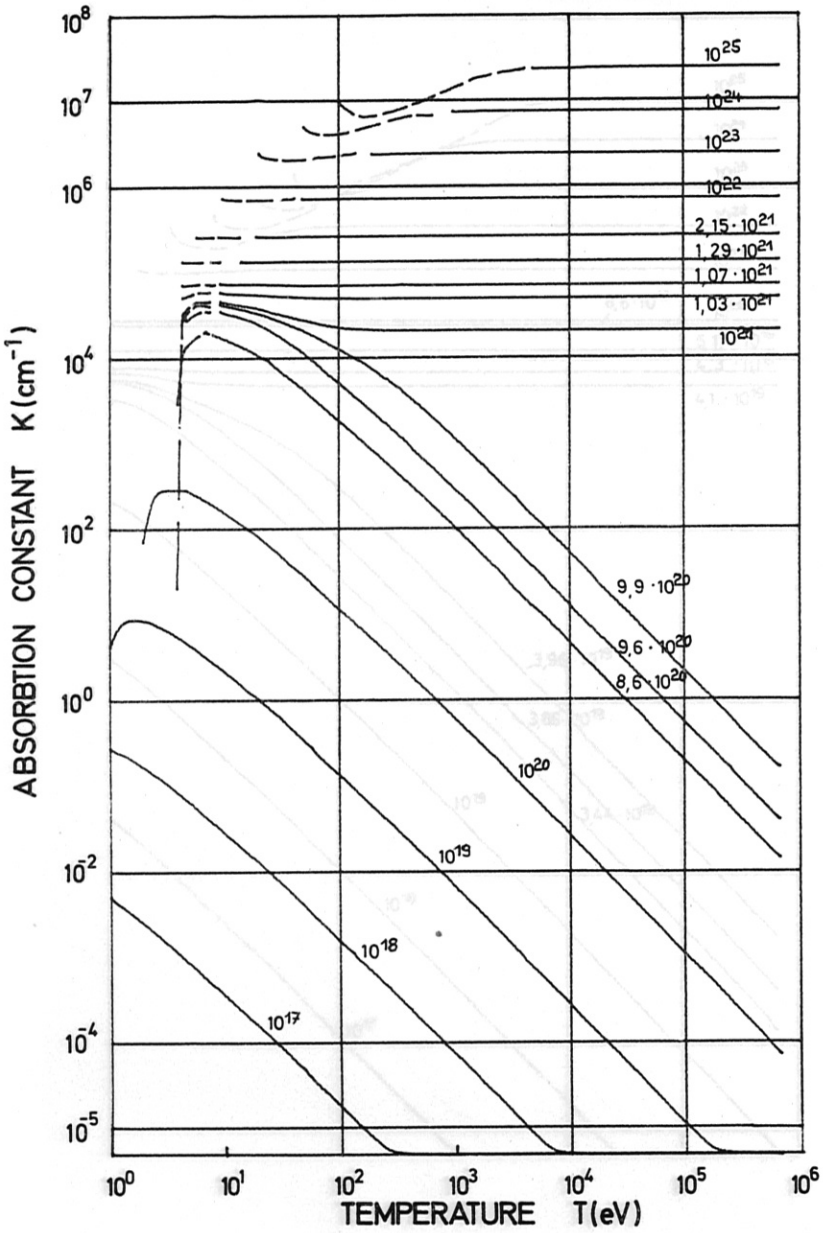

Fig. 39 Absorption constant K for the second harmonics of neodymium glass laser radiation as a function of the electron temperature T and atomic densities N for full ionization with Z = 4 (beryllium).

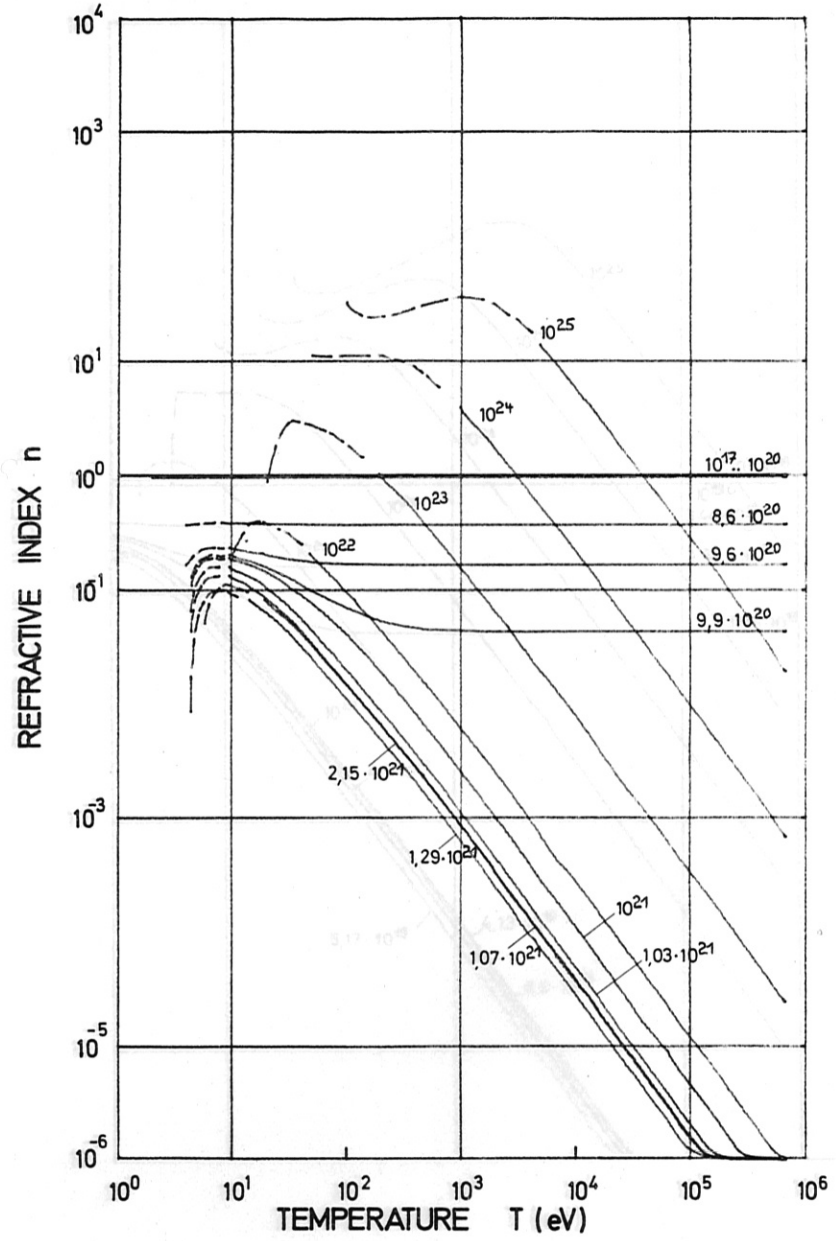

Fig. 40 Refractive index n for the second harmonics of neodymium glass laser radiation as a function of the electron temperature T and atomic densities N for full ionization with Z = 4 (beryllium).

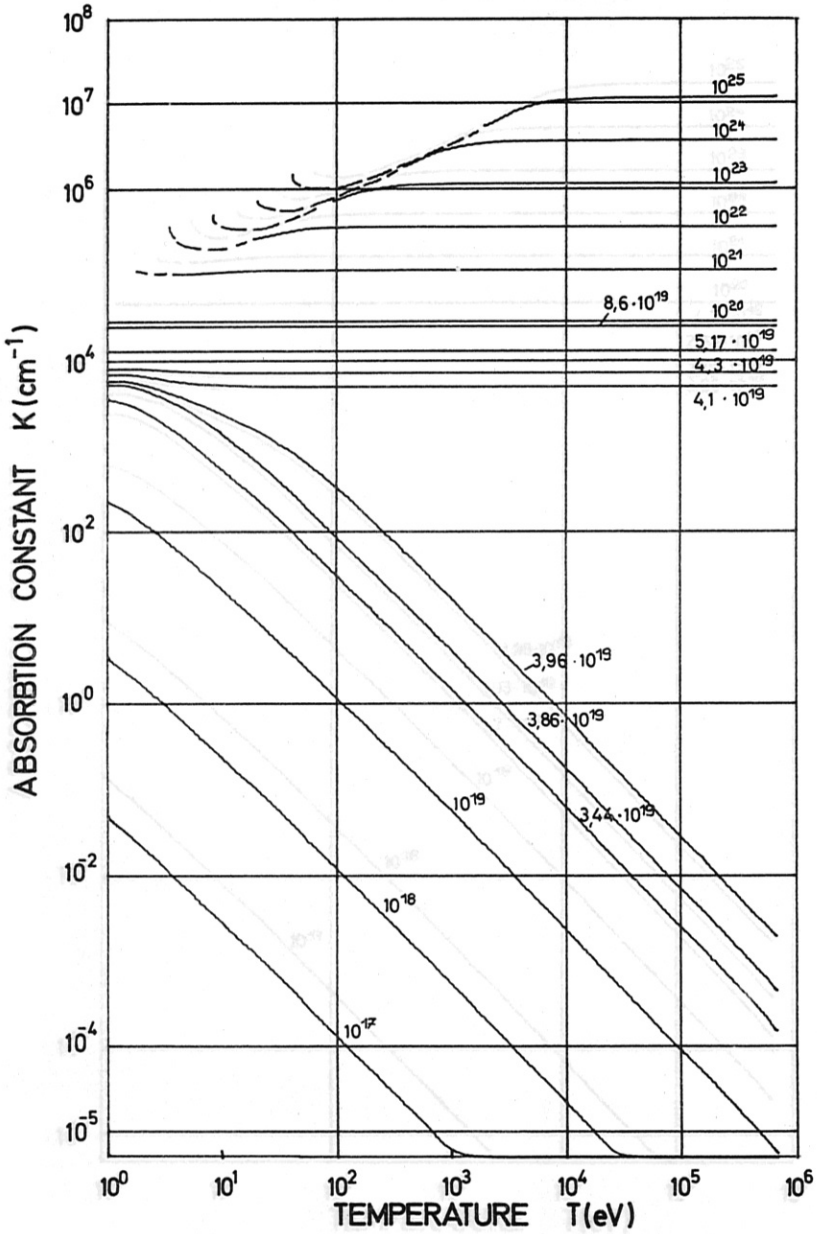

Fig. 41 Absorption constant K for the second harmonics of CO_2 laser radiation as a function of the electron temperature T and atomic densities N for full ionization with Z = 1 (hydrogen).

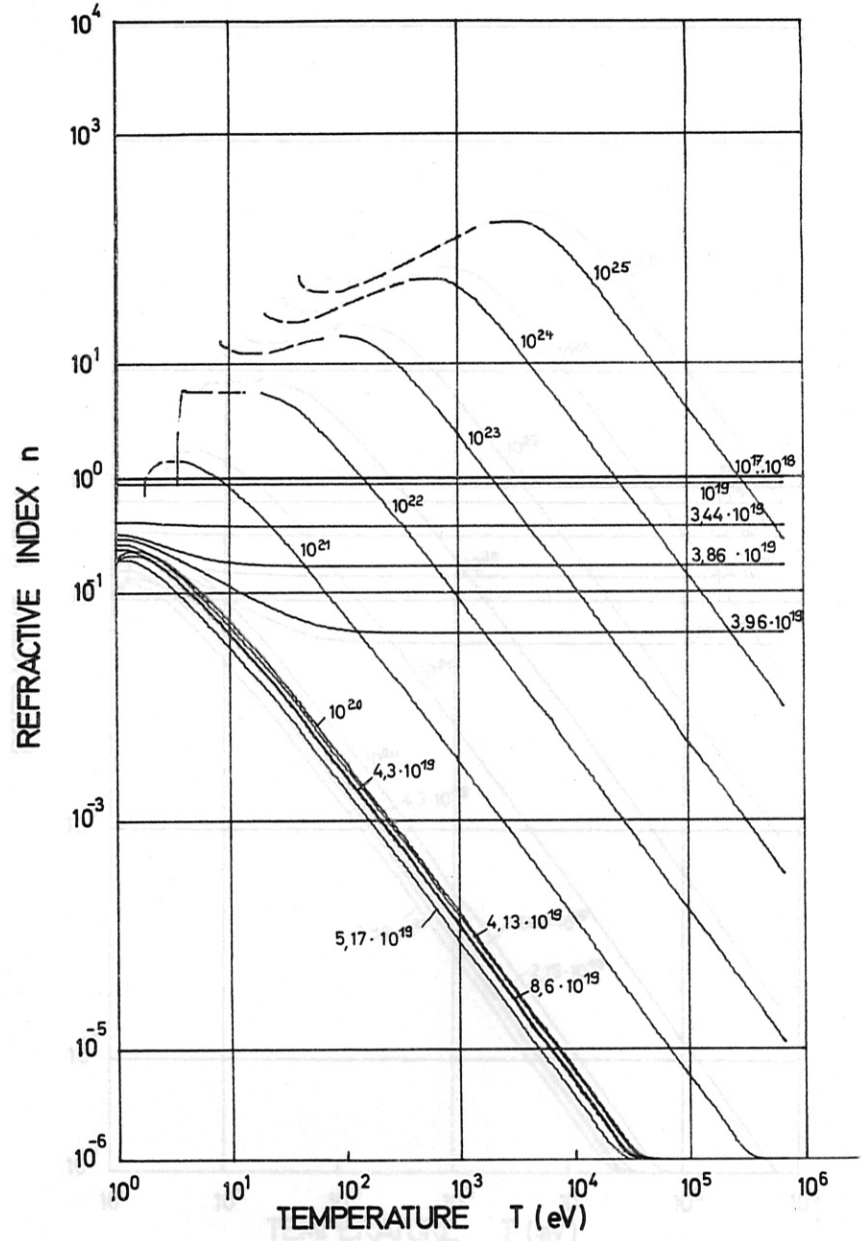

Fig. 42 Refractive index n for the second harmonics of CO_2 laser radiation as a function of the electron temperature T and atomic densities N for full ionization with Z = 1 (hydrogen).

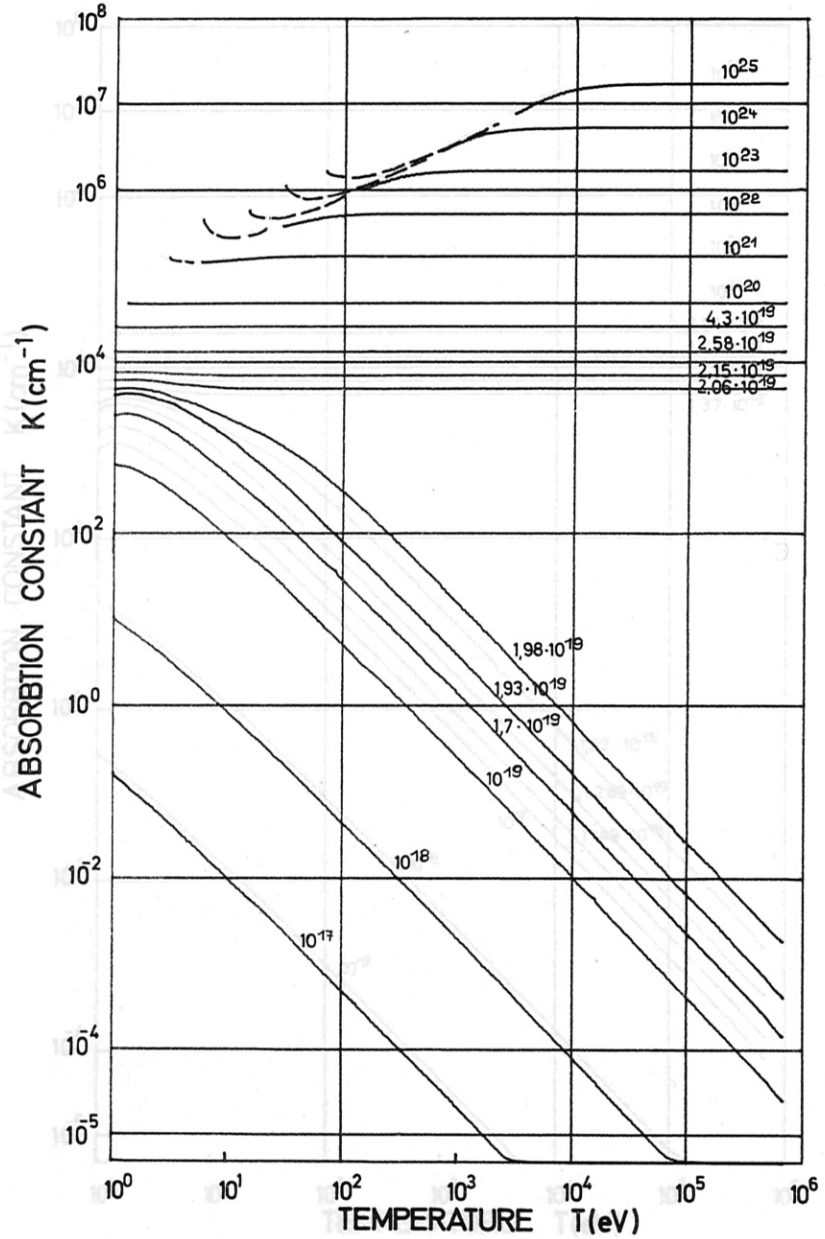

Fig. 43 Absorption constant K for the second harmonics of CO_2 laser radiation as a function of the electron temperature T and atomic densities N for full ionization with Z = 2 (helium).

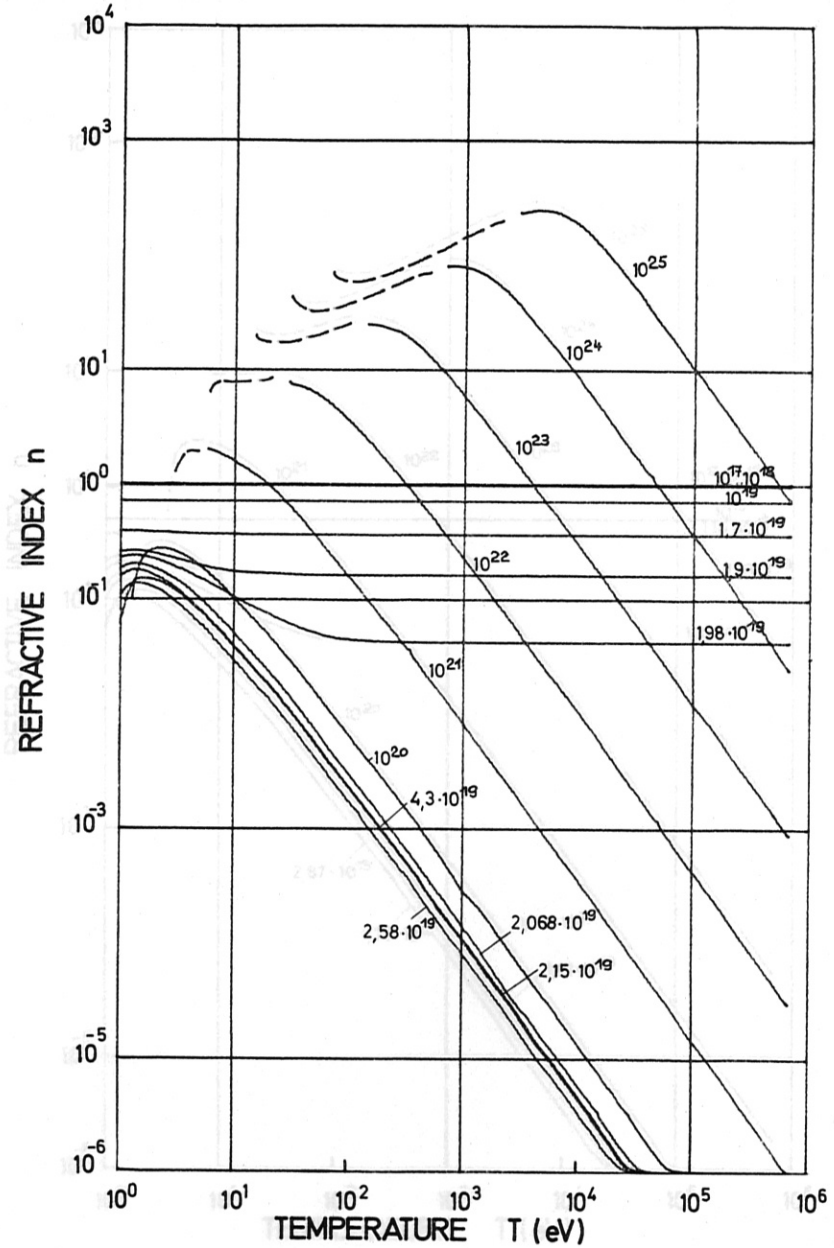

Fig. 44 Refractive index n for the second harmonics of CO_2 laser radiation as a function of the electron temperature T and atomic densities N for full ionization with Z = 2 (helium).

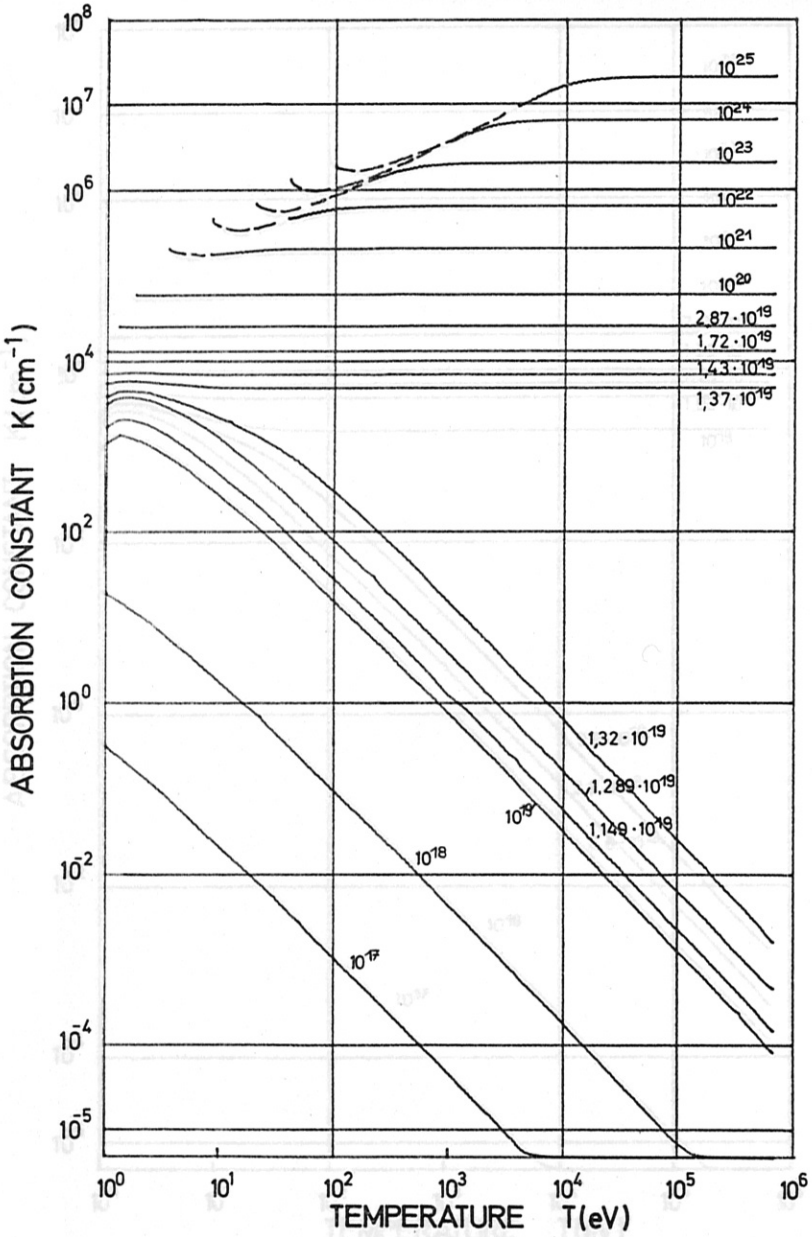

Fig. 45 Absorption constant K for the second harmonics of CO_2 laser radiation as a function of the electron temperature T and atomic densities N for full ionization with Z = 3 (lithium).

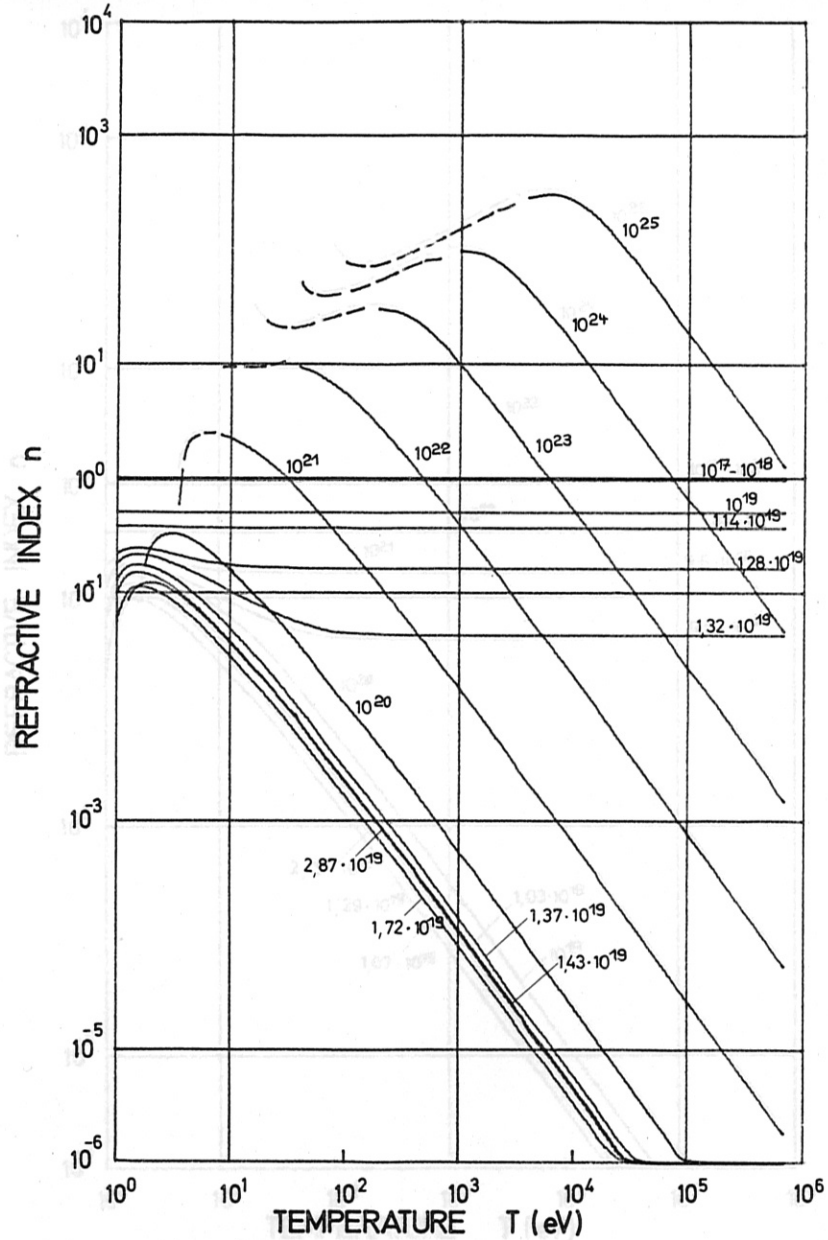

Fig. 46 Refractive index n for the second harmonics of CO_2 laser radiation as a function of the electron temperature T and atomic densities N for full ionization with Z = 3 (lithium).

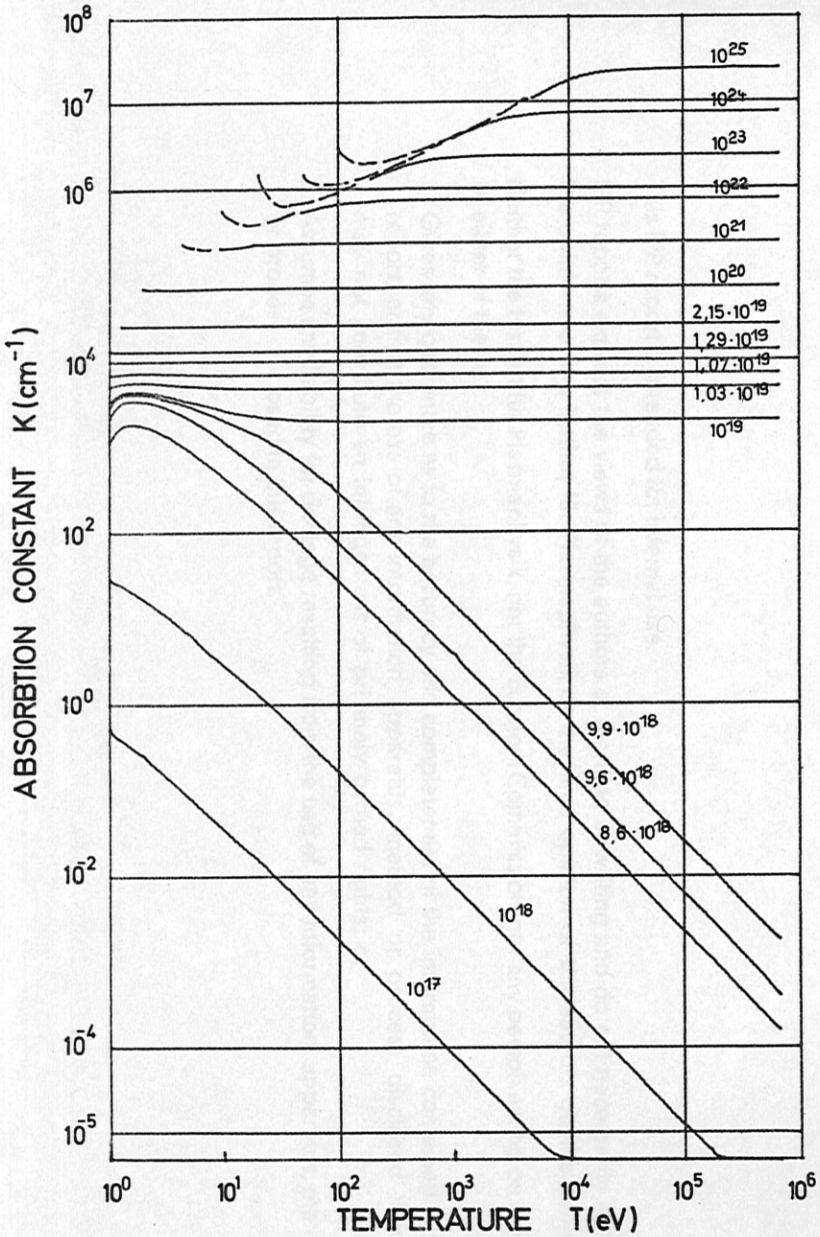

Fig. 47 Absorption constant K for the second harmonics of CO_2 laser radiation as a function of the electron temperature T and atomic densities N for full ionization with Z = 4 (beryllium).

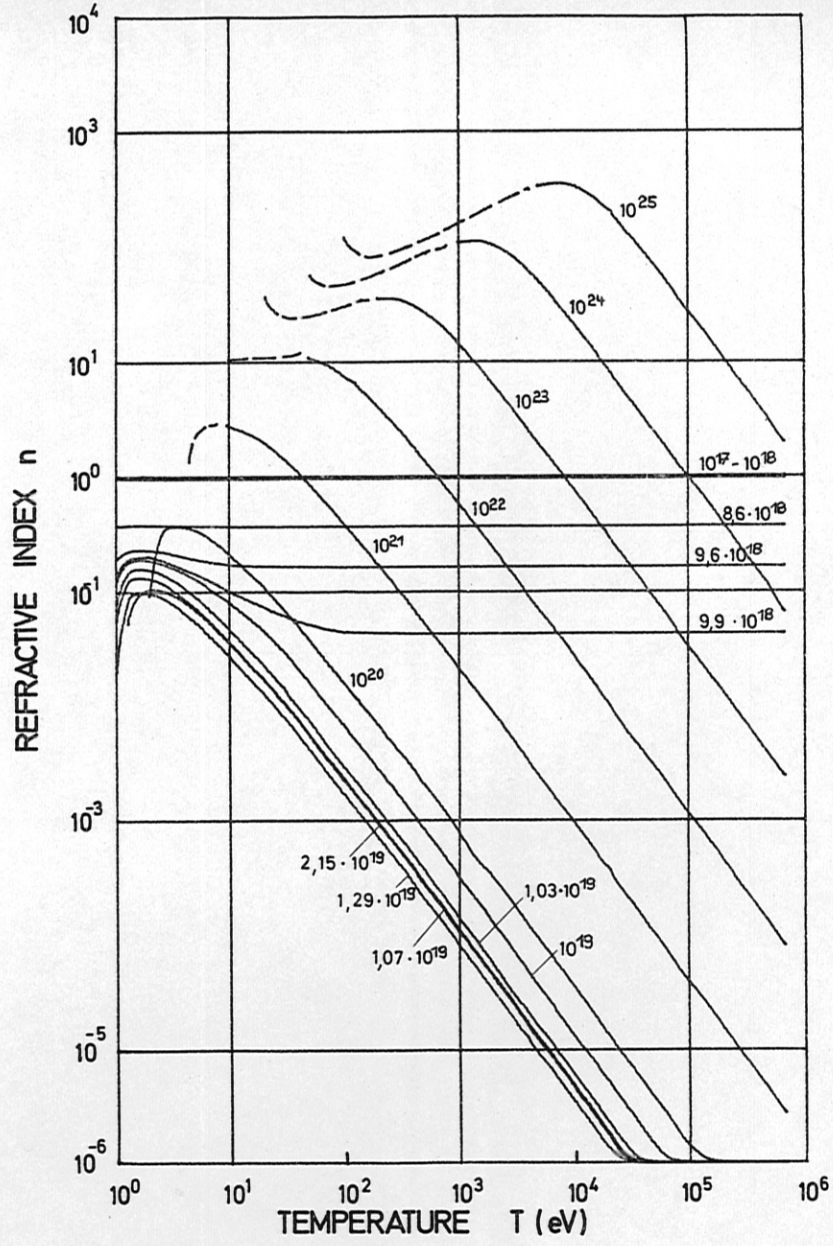

Fig. 48 Refractive index n for the second harmonics of CO_2 laser radiation as a function of the electron temperature T and atomic densities N for full ionization with Z = 4 (beryllium).